HAL
archives-ouvertes.fr

Detection of Retinal Abnormalities in Fundus Image Using CNN Deep Learning Networks

Mohamed Akil, Yaroub Elloumi, Rostom Kachouri

▶ **To cite this version:**

Mohamed Akil, Yaroub Elloumi, Rostom Kachouri. Detection of Retinal Abnormalities in Fundus Image Using CNN Deep Learning Networks. Elsevier. State of the Art in Neural Networks, 1, Ayman S. El-Baz; Jasjit S. Suri, In press. hal-02428351

HAL Id: hal-02428351

https://hal-upec-upem.archives-ouvertes.fr/hal-02428351

Submitted on 12 Jan 2020

HAL is a multi-disciplinary open access archive for the deposit and dissemination of scientific research documents, whether they are published or not. The documents may come from teaching and research institutions in France or abroad, or from public or private research centers.

L'archive ouverte pluridisciplinaire **HAL**, est destinée au dépôt et à la diffusion de documents scientifiques de niveau recherche, publiés ou non, émanant des établissements d'enseignement et de recherche français ou étrangers, des laboratoires publics ou privés.

Chapter #.

DETECTION OF RETINAL ABNORMALITIESIN FUNDUS IMAGE USING CNN DEEP LEARNING NETWORKS

Mohamed Akil[a (*)], Yaroub Elloumi[a,b,c] , Rostom Kachouri[a]

[a]Gaspard Monge Computer Science Laboratory, ESIEE-Paris, University Paris-Est Marne-la-Vallée, France.
[b]Medical Technology and Image Processing Laboratory, Faculty of medicine, University of Monastir, Tunisia.
[c]ISITCom Hammam-Sousse, University of Sousse, Tunisia.

[(*)] Corresponding author
Name and email: Mohamed Akil (mohamed.akil@esiee.fr),), Yaroub Elloumi (yaroub.elloumi@esiee.fr), Rostom Kachouri (rostom.kachouri@esiee.fr.

Abstract

The World Health Organization (WHO) estimates that 285 million people are visually impaired worldwide, with 39 million blinds. Glaucoma, Cataract, Age-related macular degeneration, Diabetic retinopathy are among the leading retinal diseases. Thus, there is an active effort to create and develop methods to automate screening of retinal diseases. Many Computer Aided Diagnosis (CAD) systems for ocular diseases have been developed and are widely used. Deep learning (DL) has shown its capabilities in field of public health including ophthalmology. In retinal disease diagnosis, the approach based upon DL and convolutional neural networks (CNNs) is used to locate, identify, quantify pathological features. The performance of this approach keeps growing. This chapter, addresses an overview of the used methods based upon DL and CNNs in detection of retinal abnormalities related to the most severe ocular diseases in retinal images, where network architectures, post/preprocessing and evaluation experiments are detailed. We also present some related work concerning the Deep Learning-based Smartphone applications for earlier screening and diagnosisof retinal diseases.

Keywords: Deep Learning, Convolutional Neural Networks, Ocular diseases screening, detection, diagnosis, classification, Smartphone applications

1. Introduction

The WHO estimates that 285 million people are visually impaired worldwide, with 39 million blinds [1]. The main retinal diseases are Glaucoma, Cataract, Age-related macular degeneration (AMD), Diabetic retinopathy (DR), Retinitis pigmentosa, Pterygium and Ocular surface neoplasia. There are several causes that contribute to increase the risk of progression and development of these diseases such as family story and genetics, diabetes, obesity, smoking, cardiovascular disease, aging, etc. Therefore, the Dry macular degeneration (Dry AMD) may first develop in one eye and then affect both. The increase of dry AMD stage damages the form of the eye. This progression is known as neovascular AMD or wet macular degeneration. For Glaucoma, the Open-angle glaucoma (OAG) is the most common form of glaucoma. The nuclear cataracts are the most common type of the cataract disease. The DR is a major complication of diabetes and Nonproliferative DR is the most common type of DR. Glaucoma, AMD, Cataract and DR are the major causes of blindness worldwide [2–5]. However, most ocular diseases affect both eyes and 80% of all causes of visual impairment are preventable or curable [1] in early stages. Late stages on ocular pathologies lead always to severe damage on visual acuity and may be irreversible such as the wet AMD. Therefore, early screening, detection and diagnosis of these ocular diseases are important for slowing down and preventing total vision loss.

Nevertheless, early screening is not ensured due to the lack of ophthalmologist where important waiting times are registered specially in industrialized countries. Moreover, patient mobility is a limiting factor in particularly of aging patients. Thus, there is an active effort to create and develop methods to automate screening of retinal diseases. Many CAD systems have been expanded and are widely used for diagnosing ocular diseases [6].

In addition, a variety of imaging modalities been developed to capture the anatomic structure of the eye. The principal imaging technologies for the retina, are scanning laser ophthalmoscopy (Scanning laser ophthalmoscope - SLO) [7] and Optical Coherence Tomography (OCT) [8] and fundus imaging technique [9] which is the commonly used to capture retinal images by fundus camera. Retinal fundus imaging provides a noninvasive tool currently used in ophthalmology.

Thus, some CAD systems based on retinal analysis were developed, extracting the anatomic structures in retinal images, such as vessel segmentation [10], detecting lesions related to DR [11], diagnosing glaucoma [12, 13], AMD [14] and cataract [15].

The fundus image is direct optical capture of the eye. This image includes the anatomic structures like Optic Disc (OD), macula regions, vasculature, blood vessels, lesions such as Red lesions, comprising microaneurysms, hemorrhages, bright lesions, such as exudates, cotton wool spots, or drusen and vascular abnormalities (see figure 1 and figure 2) by detecting microvasculature changes.

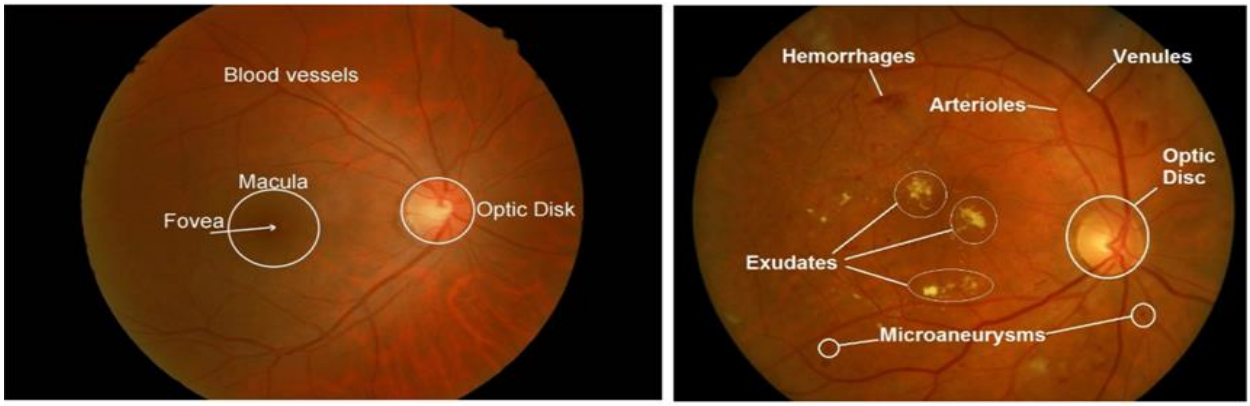

Figure 1. shows retinal morphologies (or structures), i.e. Optic Disc, Macula, Fovea, Blood vessels and abnormalities (Exudates, Microaneurysms, Arteiodes, Venules) in a fundus image.

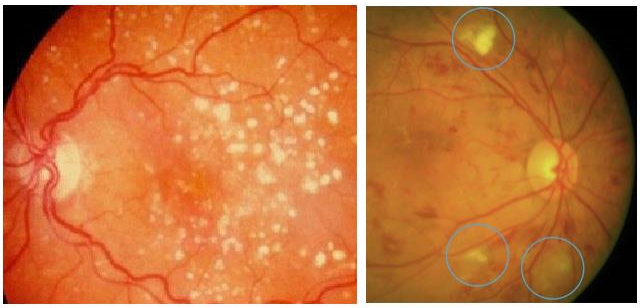

Figure 2. Two abnormalities: Hard drusen (left) and Cotton wool spots (right).

In assessing ophthalmologic disease pathologies, segmentation of retinal morphology plays a key role and has numerous applications such as OD, Cup, Optic Nerve Head (ONH) segmentation, retinal blood vessel segmentation, lesions segmentation and detection based on fundus image. The OCT modality (see an illustration in figure 3) is used for segmenting retinal layer of macula and various layers as Inner Nuclear Layer (INL), Outer Nuclear Layer (ONL), Router Plexiform Layer (OPL) and Retinal Nerve Fiber Layer (RNFL), etc.

Figure 4 shows image fundus of blood vessels and ONH capturing by Camera AFC-330.

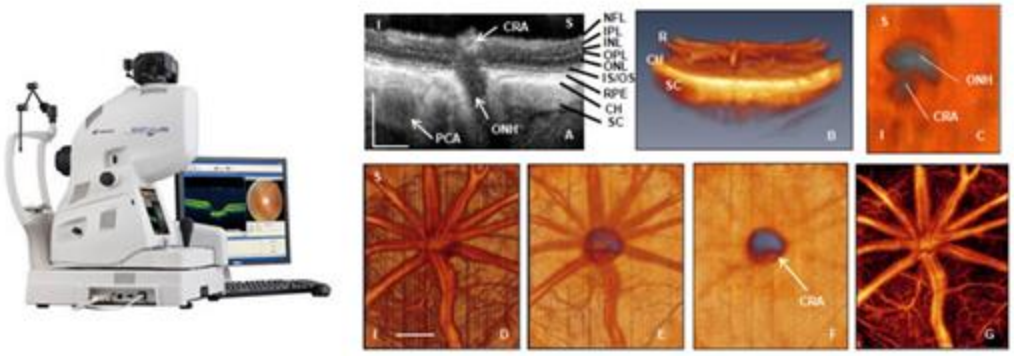

Figure 3. Topcon 3D OCT-2000 w/Digital Non-Mydriatic Retinal Camera and OCT structural image showing layers and ONH anatomy, rat central retinal artery (CRA), choroidal microvasculature.

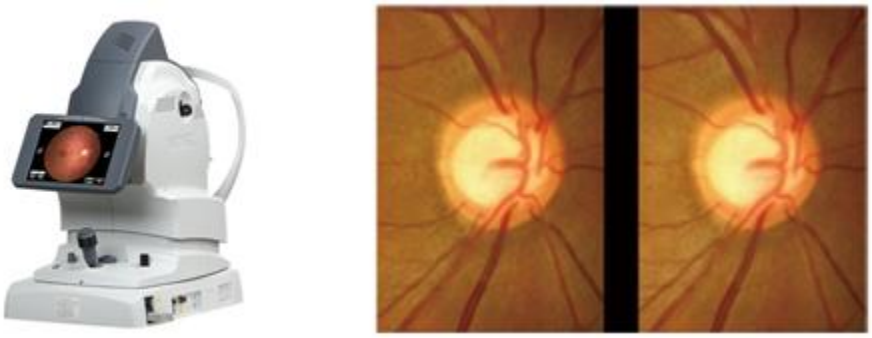

Figure 4. Non-Mydriatic Auto Fundus Camera AFC-330 and image fundus of ONH with Optic Nerve Head and Blood vessels.

The automated methods based on image analysis for ocular diseases diagnosis from both fundus and OCT images have been explored extensively. The overall block diagram of this category of methods involves two main stages. The first one is features extraction that includes several steps which are fundus image acquisition, image enhancement, Region of Interest (RoI) extraction of OD, macula, or fovea, feature extraction of disease like geographic atrophy, drusen, and feature selection. This first stage is generally based on image processing techniques for image enhancement, segmentation of the retinal structures such as retinal vessels, fovea, OD, segmentation of abnormalities like hemorrhages, microaneurysms, neovascularizations, cotton wool spots, drusen, yellow pigmentation, and detection of retinal vessels and lesions like the bright lesions. and the red lesions.

The second main stage is the ocular diseases classification into disease stage, disease type, and screening. In classification, different and most known supervised and unsupervised learning algorithms called “traditional machine learning” algorithms involving Naïve Bayes, FLD (Fisher Linear Discriminant), SVM (Support Vector Machines), KNN (k-Nearest-Neighbors), Random forests, GBDT (Gradient Boosting Decision Tree), etc. Some methods require post-processing stage.

The performance evaluation of this category of methods called in the literature “traditional methods” is done on different public and/or private datasets, using the labels provided by experts for each fundus image of the database. Different performance measures such as ACC (ACCuracy), Sen (Sensitivity) Spe (Specificity) are used to evaluate the performance of the proposed methods.

Many CAD systems and methods of ocular diseases diagnosis are reviewed in [6]. The period of the works surveyed in this paper is from 1995 to 2014. The publication trends which indicate a growing of studies using retina fundus modality and the most studied diseases are DR, Glaucoma, AMD and cataract. DR and Glaucoma are among the most important.

In the following, we report some works showing all the diversity of the methods used and especially in the classification stage.

Xiao hui Zhang et al. [11] proposed a DR diagnosis method concentrating on bright and dark lesions detection. Fuzzy C-Means algorithm is used to improve the segmentation step. The classification of the three levels (i.e. no DR, mild DR and severe DR) and dark abnormalities is done using a linear classifier model like SVM. The first step of the proposed method is an image preprocessing including Green Channel Extraction, Fuzzy Filtering, and Fuzzy Histogram Equalization to improve the image quality. The preprocessing step is followed by the retinal structure extraction step including OD localization, blood vessels detection, macula and fovea detection; The features Extraction step is dedicated to Exudate and Maculopathy detection. The last step is features classification.

To train and classify the extracted features into their respective classes, the classification stage involves several machine learning algorithms such as k-NN, polynomial Kernel SVM, RBF Kernel SVM, Naïve-Bayes. The average results of the accuracy when using the four classifiers k-NN, Polynomial Kernel, SVM RBF Kernel, SVM Naive Bayes are 0.93, 0.7, 0.93, and 0.75 respectively.

Jôrg Meier et al. [12] described an automated processing and classification for Glaucoma detection from fundus images. In particular, the effects of the preprocessing on classification results have been studied. In particular, non-uniform illumination is corrected, blood vessels inpainting is used and the RoI is normalized before features extraction and classification. The features are computed by the Principal component analysis (PCA). Then, SVM is used for features classification. The PCA provides a classification success rate of 81%.

A. Mvoulana et al. [13] proposed a fully automated methodology for glaucoma. Their method provides an OD detection method, combining a brightness criterion and a template matching technique, to detect the OD as a RoI and segment the OD and OD. The CDR clinical feature is computed and then used for binary classification thus obtained two classes (i.e. healthy and glaucomatous patients). The publicly available DRISHTI-GS1 dataset is used to evaluate the performance of the proposed method achieving 98% of accuracy on final glaucoma screening and diagnosis.

Mookiah et al. [14] addressed an automated AMD detection system. The proposed system incudes fundus image acquisition, preprocessing, Discrete Wavelet Transform (DWT), feature extraction, feature ranking and selection, and classification. Various feature ranking strategies have been used like t-test, KLD (Kullback-Lieber Divergence), CBBD (Chernoff Bound and Bhattacharyya Distance) to identify an optimal feature set. A set of supervised classifiers namely SVM, DT (Decision Tree), k-NN, Naive Bayes (NB) and Probabilistic Neural Network (PNN) were used to measure the best performance which uses a minimum number of features. The classification provides normal and dry AMD.

KLD ranking and SVM Classifier provide the best performance with an average accuracy of 93.70%, sensitivity of 91.11% and specificity of 96.30%.

In [15], Liye Guo et al. proposed a framework of cataract classification and grading from image fundus as an input. Their framework includes fundus image pre-processing, feature extraction, and automatic cataract classification and grading. The feature extraction method is based on the sketch method with discrete cosine transform. For classification and grading of cataract disease, a multi-class discriminant analysis is applied. For training and testing, the proposed framework uses 445 fundus image samples as dataset including fundus image samples with mild, moderate, and severe cataract grades. This dataset is real-world one. The classification rate in cataract or non-cataract classes is 90.9%. For cataract grading in nuclear cataract, or cortical cataract or posterior sub-capsular cataract grade, the classification rate is equal to 77.1%.

These methods under-perform due to variations in image properties and quality such as non-uniform illumination, small size of the objects in retinal imaging. Also, the technical specifications and conditions use of the fundus camera, resulting from the use of varying capture devices are the important causes of deterioration of the performance of these methods. We can note that robustness and accuracy of the used approaches for RoI detection and segmentation of the retinal structures (i.e. Optic Disc, Cup, Nerve Head, Blood vessel, drusen, red lesions, microaneurysms, hemorrhages, exudates, retinal neovascularization) play a major role in terms of performance. DL and CNN has shown its abilities in different health domains including ophthalmology [16]. DL and CNN can identify, localize, quantify and analyze the pathological features and diagnose the retinal diseases. The performance of the approach based upon DL and CNN keeps growing.

In this chapter we will give an overview of the use of CNN Deep Learning Networks in detection of retinal abnormalities using retinal images as shown in figure 5.

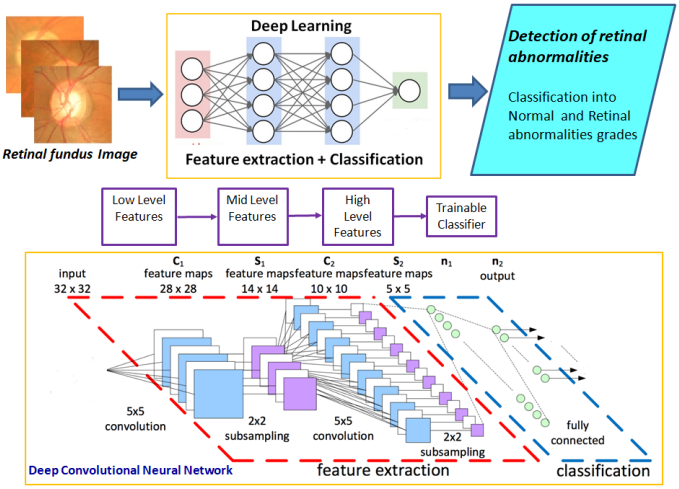

Figure 5. Illustration of deep learning model (fully "end-to-end" learning) for both feature extraction and classification from retinal fundus image as an input.

We will focus on earlier screening and diagnosis of glaucoma, AMD, DR and cataract diseases. In particular, we will report the related works based on Hybrid and fully methods. The hybrid method employs both image processing for preprocessing and post processing steps and deep learning for feature segmentation and classification with CNN Deep Learning Networks. In fully method, CNN Deep Learning Networks is used for feature extraction step and classification from the input directly. Two types of retinal imaging modalities will be considered, OCT and fundus camera for capturing fundus images as inputs for the CAD System based upon CNN Deep Learning network.

The section 2 presents an overview of existing methods of earlier screening and diagnosis of ocular diseases using CNN Deep Learning Networks. In this section we describe the CNN Deep Learning Networks based approaches related to Glaucoma, AMD, DR and Cataract diseases. In section 3, we present some related work concerning the Smartphone applications based on DL for detection of retinal abnormalities. Section 4 is the discussion and Section 5 gives the conclusion.

2. Earlier screening and diagnosis of ocular diseases with CNN Deep Learning Networks

Several ocular pathologies may affect retinal components and features (see section 1), which causes abnormalities and lesions like exudates or hemorrhages in the retina. In this section, we consider the most severe ocular diseases and we focus on existing methods of earlier screening and diagnosis of these diseases. A summary report of the recent work carried out on CNN Deep Learning Networks methods is provided.

2.1. Glaucoma

2.1.1. Methods and Materials

Glaucoma is a neurodegenerative chronic ocular pathology that alters nerve fibers and hence leads to damage progressively the neuro-retinal rim and the optic nerve head (ONH) [17]. It consists at significant rise of intraocular pressure [18]. Moreover, it occurs to clustering vessels in the border of Optic Disc (OD). Figure 6 shows two examples of this retinal disease.

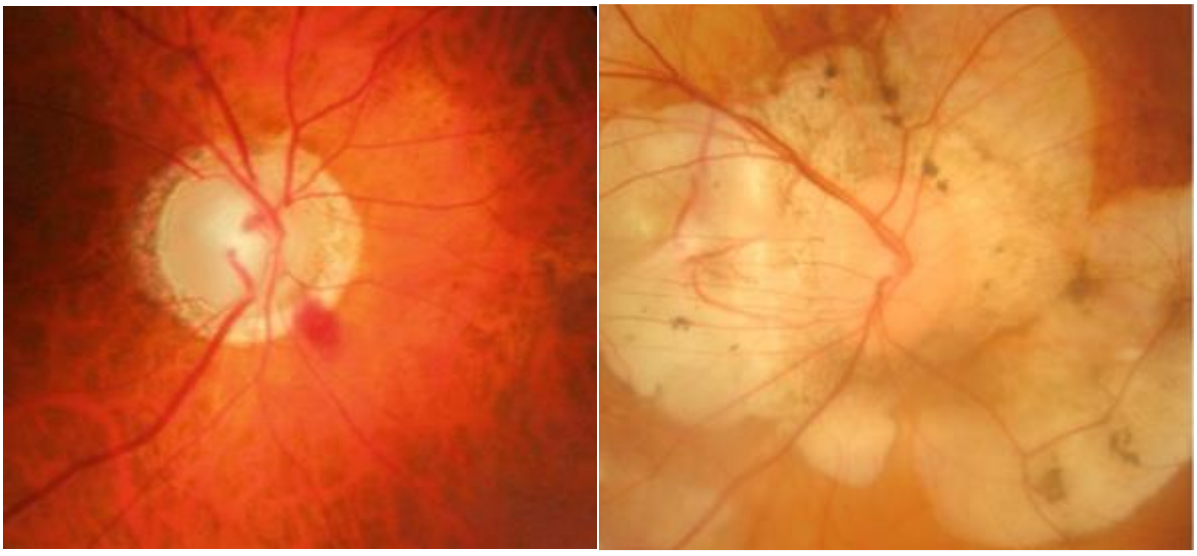

a b

Figure 6. Presence of glaucoma [19]: (a) early signs of glaucoma and (b) advanced stage of this eye disease.

The two main types of this disease are open-angle glaucoma and angle closure glaucoma. About 90% of the affected people suffer from primary open-angle glaucoma [20].

Current open-angle glaucoma detection has been established in a community-based healthcare system, and it is heavily dependent on accessibility to qualified ophthalmologists, optometrists, or general practitioners for clinical examination as well as dedicated ophthalmic testing equipment, including tonometer's, automated perimetry, and disc photography or OCT. The early stage of glaucoma does not generate symptoms or changes to the visual field [18]. However, this neuropathy is highlighted by a progressive lack of vision sensitivity, potentially, if not treated, leading to blindness at term [21].

Indeed, the glaucoma disease leads to shift blood vessels in the optic disc region. Moreover, bifurcations and their angles are adjusted with respect to the excavation. In addition, grouping vessels leads to superimpose them where may be modeled as unique vessel in the fundus image. Glaucoma is known as affecting a significant part of the population worldwide, with more than 64 million cases globally reported in 2013, and estimations reaching 80 million and 111.8 million cases respectively by 2020 and 2040 [17, 22, 23]. Given the irreversible nature of glaucomatous optic nerve degeneration combined with increased longevity of the population, early diagnosis is important to prevent severe visual morbidity and the associated healthcare and society burdens [24].

Traditionally glaucoma is diagnosed by measuring the IOP with a tonometer, and rating an abnormal high-pressure rate, which is not always a reliable and sufficient criterion for glaucoma assessment [25, 26]. Otherwise, glaucoma can be diagnosed within the assessment of the ONH. The ONH is the region in the retina where blood vessels converge, it is composed of a bright circular region called the optic disc (OD), and inside the OD, a brighter region called the optic cup (OC) is apparent.

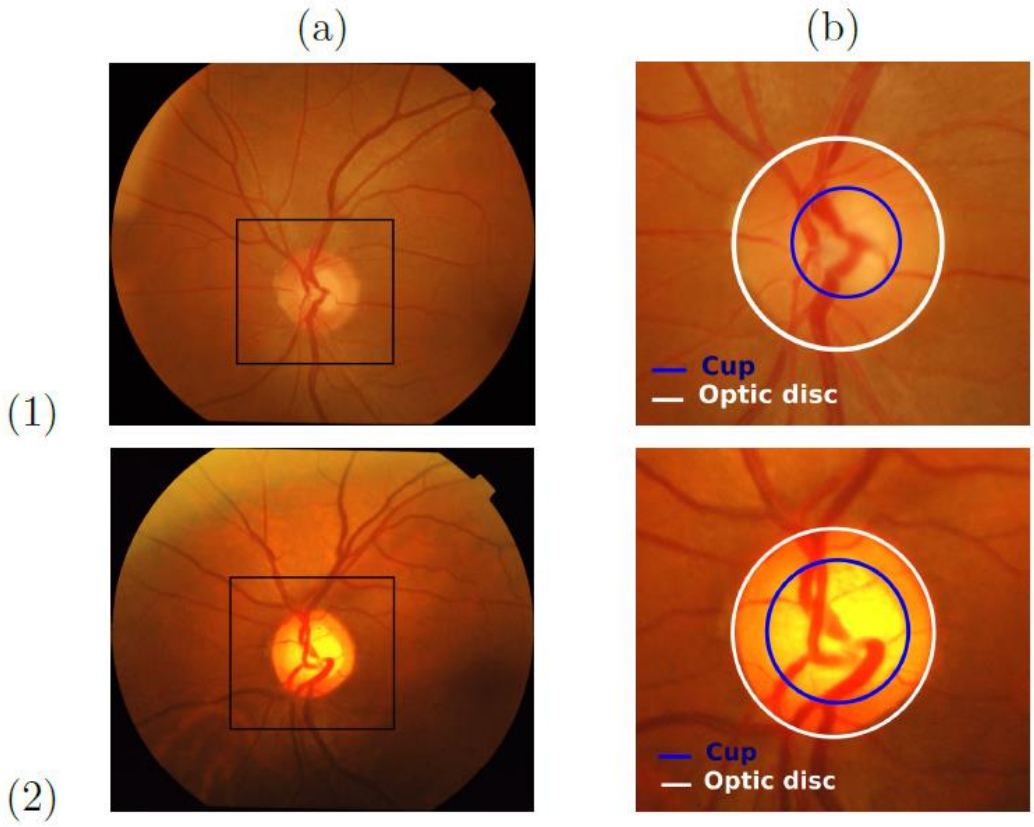

Figure 7. Example of healthy (1) and glaucomatous (2) retinal images [13]: (a) Retinal image with framed optic disc (OD) region around the ONH, (b) OD sub-image with OC and OD areas.

In Figure 7, two retinal images are presented, showing a sub-window around the ONH, with each of the OD and OC borders. Glaucoma goes with ONH appearance changes, as the OC region becomes more prominent as shown with both healthy (1) and glaucomatous (2) cases.

In this direction, retinal image study can be applied for glaucoma screening [10]. Many works have been conducted offering more accuracy on the final diagnosis, less workload for the specialist, and useful mass screening programs. Detecting the presence of the disease from retinal images consists in assessing the ONH and the retinal nerve fiber layer (RNFL), by extracting indicators such as the Cup-to-Disc Ratio (CDR) [28], the Inferior Superior Nasal Temporal (ISNT) rule [29], the RNFL thickness [30], parapapillary atrophy [31] or ONH hemorrhages [30].

In the last decade, deeplearning has been extensivelyapplied for ophthalmic diagnosticsachieving good results on various fundus and OCT datasets. Optic Disc, Cup and Nerve Head Segmentation is an important step for automatic cropping of the region of interest for furtherprocessing [32].

2.1.2. Deep-Learning neural-network architectures for glaucoma screening and diagnosis

The first implementation of deep learning architecture in OD segmentation was proposed by Lim et al. [33] in 2015. The proposed CNN is developed for calculatingcup-to-disc ratio as a measure of the presence of glaucomausing MESSIDORand SEED databases. The most probable localized region around OD was chosen using Daubechies wavelet transform. Due to the presence of noise, the probability of a pixel to be inside or outside of the OD region was calculated. This methodachieved an AUC = 0.847.

In [34] the authors segmented both OD and OC separately.

Edupuganti et al. [35] used Drishti-GS to implement one shot segmentation pipeline for segmenting OD and OC for glaucoma analysis. FCN with VGG16 encoder-decoder was used and convolution was performed with a stride of 8 pixels. Due to a limited number of training images, ImageNet (http://www.image-net.org/) was used for initialization of the FCN encoder. This is a case of transfer learning which broadly falls under the section of domain adaptation where parameters from a trained model are used to test on a different dataset to reduce the need of huge amount of training data. After augmentation 160 images were used for training, 10 for validation and 50 for testing. As a result highest mean accuracy achieved was 88.23%, and Fscores of segmenting cup and disk were 0.897 and 0.967 respectively.

Zilly et al. [36] propose a method using an ensemble learning based convolutional neural network architecture. This method is used to segment the optic cup and optic disc from retinal fundus images. As a clinical outcome indicator of the glaucoma, the CDR is calculated and used to obseve the behavior changes of the galucoma progression. The proposed method is computationnaly efficient, provinding an accurate and robut segmentation.

More recently Liu et al. [37] used fundus images to implement deep learning based segmentation architectures to segment glaucomatous OD. The authors collected 3768 fundus images from 3 ophthalmology clinics in Australia, and also used images from RIM-ONE and HRF.

For locating and estimating the size of OD difference-of-Gaussian blob detector was employed with enlarging kernel size Gaussian filter to input images. Pixel wise consecutive image differences were calculated to get n-1 Gaussian maps for n input images. ResNet50 model was implemented with 48 full convolutional neural network layers. A previously trained model with ImageNet database was used and the output layer was replaced by a new output layer with 2 nodes for 2 different classes normal and glaucoma. For disc segmentation, 3200 images were used for training. The model achieved an accuracyof 91.6% for disc identification, with an AUC of 0.97 when applied to 800 test images. On HRF dataset it achieved 86.7% sensitivity and specificity. In contrast with the previous works, this work gathered a larger amount of data from different sources with different image qualities and resolutions. Hence this model can be considered as more robust than most of the other works.

2.1.3. Application and evaluation on earlier glaucoma screening and diagnosis – classification

2.1.3.1. Fundus image Glaucoma Classification

One of the early publications in glaucoma classification usingdeeplearningwas by Chen et al. [38]. They implemented a CNN with dropout anddata augmentation on ORIGA and SCES datasets. A six layers deep CNN with 4 convolutional layers of progressively decreasing filter size (11, 5, 3, 3) followed by 2 dense layers was used to get 83.1% and 88.7% AUC on ORIGA and SCES respectively. Improving their previouswork, [38] Chen et al. [39] presented a model using Contextualized CNN (C-CNN) architecture. It combined the output of convolutional layers of multiple CNN to a final dense layer to obtain the softmax probabilities. The 5 C-CNN model which was a concatenation of outputs of last convolutional layers of 5 CNNs each of depth 6 (5 convolutiona llayers + 1 MLP) provided an AUC of 83.8% and 89.8% on ORIGAand SCES datasets, respectively.

Fu et al. [40] used a 3 layer deep Feed-forward Neural Network (FNN) on a private dataset of 171 Glaucoma images. It achieved an AUC of 92.6%.

Chakravarty [41] was first to propose a method for joint segmentationof OD, OC and glaucoma prediction from the REFUGE dataset. In this method CNN feature sharing for different tasks ensured better learning and over-fitting prevention. The parts of the model that were shared with U-net contained 8 times fewer number of CNN filters than the conventional U-net. It was probably done to prevent over-fitting since the study used a smaller dataset than U-net. It used an encoder network to down sample the feature and then a decoder network to restore the imagesize. Two different convolutional layers were applied on the decoder network's output for OC and OD segmentation. The OC and OD segmentation masks were merged into separate channels and CNN was applied to it. The outputs of the CNN and encoder output were combined and fed to a singleneuron to predictglaucomaachieving an AUC of 94.56%. With a lower number of parameters this method achieved comparable performance with existing architecture e.g. [42].

Zhixi et al. [43] used the Inception-v3 architecture on crowd-funded LabMe database (http://www.labelme.org/) with 48000 images to detect glaucomatous optic neuropathy. Here researchers graded the images by trained ophthalmologists befor eapplying the algorithm. Local space average color subtraction was applied in pre-processing to accommodate for varying illumination. The Inception-v3 network was used for classiffication. The large dataset in conjunction with a deep model resulted in an AUC of 98.6%.

Chan et al. [44] presented a framework on a dataset of fundus images obtained from various hospitals by incorporating both domain knowledge and features learned from a deep learning model. This method was also used in other applications [45]. The OD image provided local CNN features, the whole image provided global CNN features whereas domain knowledge features were obtained from diagnostic reports. It used a total of 25 features including 3 numerical features:intraocular pressure, age, and eye sight as well as 22 binary features such as swollen eye, headache, blurred vision and failing visual acuity.The disk and whole images were fed to two separate CNN while domain knowledge features were fed to a third branch consisting of a fullyconnected neural network. These three branches were concatenated by a merge layer followed by two dense layers and a logisticregression classifier. The model benefited from diagnostic features along with fundus images and attained an accuracy of 91.51% .

2.1.3.2. OCT image Glaucoma Classification

Muhammad et al. [42] used a hybrid of AlexNet and random forest on widefield OCT of 102 patients for glaucoma classification. The pretrained AlexNet model wasused for feature extraction from OCT images. The weights of nodes of fully connected layers of the neural net wereusedas input for the random forest classifier. Six image types for each patient were used with leave-one-out cross-validation to train the model.

A vertically flipped copy of each image was also added and nodes from fully connected layer, 6 were found to have the best accuracy of 93.1% using RNFL probability map. The method outperforms OCT and VF clinical metrics which gave up to 87.3% accuracy but fell short of 98% obtained by an experienced human expert.

Fu et. al. [27] presented multi-context deep network (MCDN) for angle closure glaucoma screening using a private dataset called Visante Anterior Segment OCT dataset. Two parallel streams were used to fine-tune a pretrained VGG-16 on the local and global image. The feature maps from these streams were concatenated at the dense layer and supplemented with clinical parameters with analysis by a linear SVM for final classification. Intensity-based data augmentation was performed instead of traditional scale based augmentation because the anterior chamber was found at a consistent position in Anterior Segment Optical Coherence Tomography (AS-OCT) images and obtained an AUC of 0.9456.

2.1.4. Datasets used in glaucoma diagnosis [32]

ACHIKO-K [46]: This database is dedicated mainly for glaucoma studies and was collected from a Korean population. In this database, there are 258 manually annotated fundus images among which 114 are glaucoma images and 144 are normal images. The online link to this dataset is https://oar.a-star.edu.sg/jspui/handle/123456789/1080?mode=full

DRIONS-DB [47]: This database consists of 110 color fundus images. Miguel Servet Hospital, Zaragossa Spain developed this dataset for optic nerve head segmentation. Among all the patients 23.1% had chronic glaucoma and 76.9% of them had eye hypertension. This dataset can be found at http://www.ia.uned.es/~ejcarmona/DRIONS-DB.html

HRF [48]: This public database contains 15 images of healthy patients, 15 images of patients with DR and 15 images of glaucomatous patients captured with Canon CR-1 fundus camera with a 45 FOV. Expert segmentations are provided for each image. This can be found publicly at https://www5.cs.fau.de/research/data/fundus-images/

SEED [49]: This database originated from a study performed by the Singapore Epidemiology of Eye Diseases. This dataset has 235 fundus images among which 43 are glaucoma images, 192 are normal images. This is not available online for public use. Singapore Chinese Eye Study (SCES) and Singapore Indian Eye Study (SINDI) databasesalso came out fromthissamestudy.

ORIGA [50]: ORIGA stands for Online Retinal Image dataset for Glaucoma Analysis, and itconsists of 650 retinal fundus images. The Singapore Eye Research Institute conducted the project and data werecollectedfrom the Singapore Malay Eye Study or SiMES over a three year period of 2004-2007. This dataset is not currently available online

RIGA [51]: RIGA is a public dataset and stands for Retinal Images for Glaucoma Analysis. This dataset mainly consists of retinal fundus images of glaucoma patients. The RIGA dataset was developed by concatenating images from MESSIDOR, and images obtained from Magrabi Eye Centre, Riyadh and Bin Rashid Ophthalmic Centre, Riyadh. There are a total of 760 retinal fundus images in the database.
This can be found at https://deepblua.lib.umich.edu/data/concern/generic_works/3b591905z

REFUGE [52]: This datasetis part of the retinal fundus glaucoma challenge organized by Medical Image Computing and Computer Assisted Intervention 2018 meeting held in Spain. This dataset has 1200 annotated fundus Images. Recently this competition also included images for AMD. This can befound at https://refuge.grand-challenge.org/

2.2. Age-Related Macular Degeneration

2.2.1. Methods and Materials

AMD is an eye disease that primarily affects the elderly. It is considered as an irreversible chronic pathology [53] and the leading cause of vision loss in people over 50 in developed countries [54]. The AMD is frequently diagnosed using a fundus image which aims to detect degenerative lesions caused by each stage. This pathology impacts the vision in two stages [55]. In the early stage, the majority of patients do not feel any symptoms. The questioning of patients may deduce that a reduction in contrast perception or discomfort in night vision appeared. In late stage, the vision is deteriorated where the shapes become progressively distorted. Thereupon, a black spot, called scotomas, appears in the field of vision where its size increases with respect to the AMD severity (see figure 8).

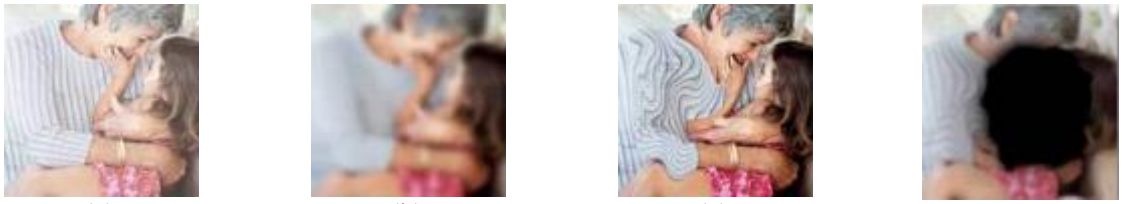

(a) (b) (c) (d)

Figure 8. visual acuity : (a) non pathologic vision; (b) early stade vision ; (c) straight line deformation ; (d) scotoma apparision [56]

The early stage is detected by identifying drusens that represent yellowish components with a higher contrast than the texture of the retina. This stage is always partitioned into to levels: the early AMD level where the drusen diameter is between 15 and 63 μm and the intermediate AMD level where the drusen diameter is between 63 and 125 μm. The late stage is characterized by a gradual decline in visual acuity. It is corresponding to the presence of drusens where their diameters are above 125 μm. Moreover, it has two different forms. For the atrophic or dry AMD or geographic atrophy (GA), the patients are generally embarrassed by a scotoma (dark task). For the exudative or wet or neovascular form, the patients notice a distorted perception of straight lines and the possible presence of a scotoma. Figure 9 give some AMDs symptoms such as (b) image fundus with drusens (figure 9.b), dry (atrophic) AMD (figure 9.c) and wet (neovascular or exudative) AMD (figure 9.d).

The number of AMD patients could reach 196 million in 2020 and 288 million in 2040 [57]. The number of patients in Europe will exceed 50 million in 2020 [58]. In France, the AMD affects 8% of the entire population. Moreover, its frequency increases with old age [58]: 1% of the population aged between 50 and 55; about 10% of the population aged between 65 and 75; and between 25% and 30% for those over 75 years of age [59].

The transition from early to late AMD always requires several years. The work described in [55] indicates that the risk of developing early stage in 5 years ranges from 0.5%to 42%.

However, AMD therapies cannot cure or reverse vision loss. They only reduce the risk of progression to late stages. Consequently, early AMD diagnosis is essential.

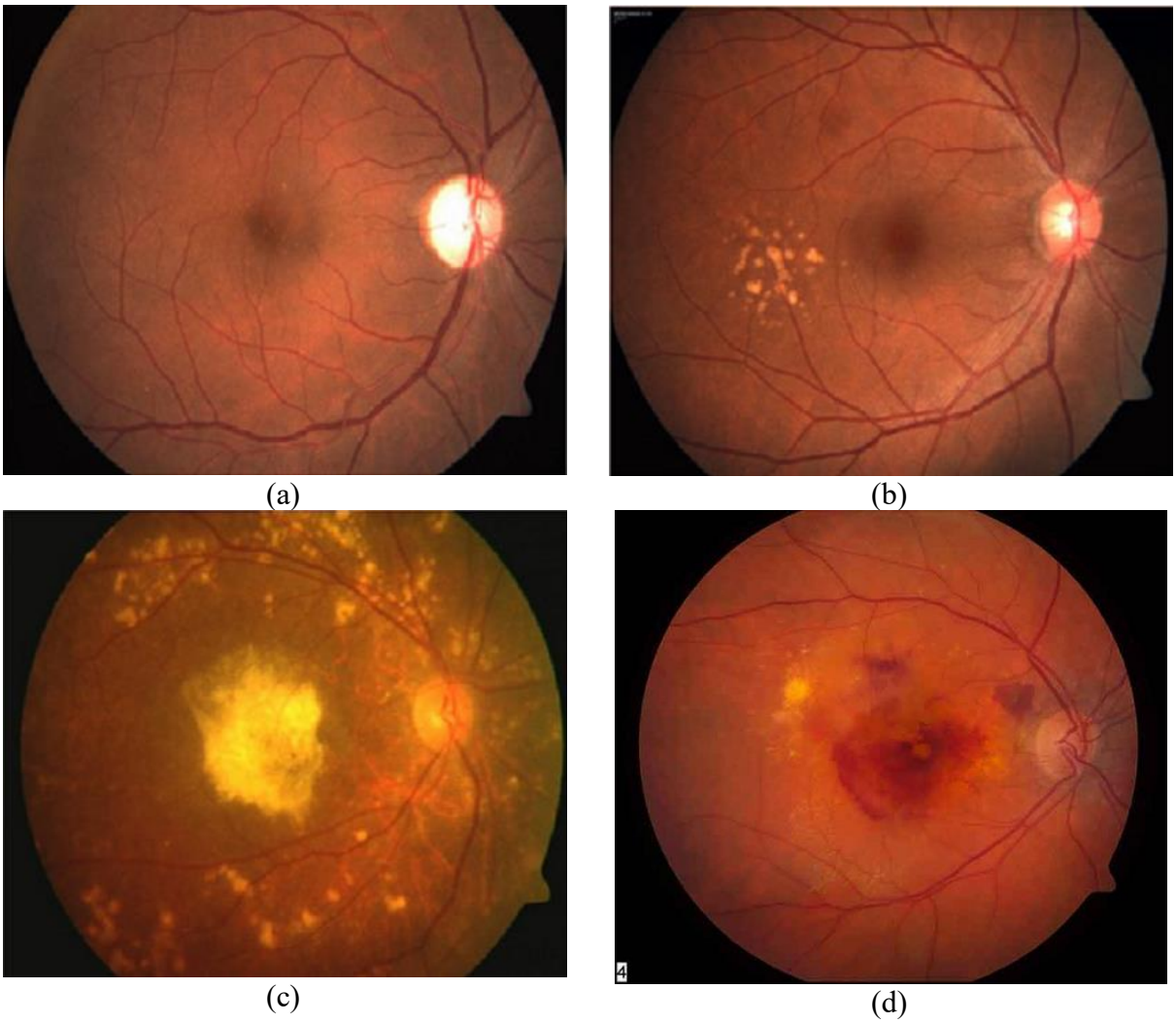

Figure 9. Example of DMAL's symptoms: (a) image fundus image of healty eye; (b) image fundus with drusens ; (c) dry *(atrophic) AMD; (d) wet (neovascular or exudative) AMD.*

The World Health Organization reports that 8 million people have a severe blindness due to the AMD. The number of patients is expected to increase to 1.5 times over the next ten years [54, 57, 58]. In France, nearly 1 million people over 50-year-old suffer from vision problems caused by AMD, with an increase of 3000 new cases of blindness each year [56]. In the international context, following the study carried out in [58], prevalence statistics of AMD in France are similar to those of industrialized countries such as the other European countries or the United States.

The treatment of early stage involves using Omega 3-based dietary supplements. For the late form, only wet AMD can be treated. The therapy is based on intravitreal injections which represents a considerable charge for medical management systems. Automatic approaches for diagnosing AMD using fundus image have been proposed in several research work. These approaches consist of locating the macula and then analyzing its texture [60, 61, 62]. There are two categories of work according to the result of the diagnosis. The first is to determine the stage of AMD [63, 64]. The second category consists of segmenting the drusens caused by AMD [65, 66].

Several studies have been provided similar performances compared to those of ophthalmologists. We deduce that some works are based on deep learning which are distinguished by their higher performances compared to previous methods.

2.2.2. Deep-Learning-based methods for AMD detection and grading

The work described in [67] proposes a 2-class classification method to diagnose AMD at an early stagebased on fourteen-layer deep Convolutional Neural Network (CNN). The network is composed by seven convolution layers, four max-pooling layers, and three fully-connected layers. The training was performed using the softmax activation function, the backpropagation « Adam » algorithm, and run during 60 epochs. The input image was resized to 180 × 180 and then augmented four times by respectivelly flipped to the left, flipped downwards, flipped to the left then downwards.

The evaluation is performed using a private dataset composed by 1110 fundus images which are split into 402 healthy, 583 with ealry, intermediate and dry AMD and 125 with wet AMD.The method validation is performed using two strategies.

A first validation strategy, called « blinfold », consists in using the same data set for either treaning and testing. The « blinfold » strategy achieves an accuracy of 0.9117, a sensitivity of 0.9266 and a specificity of 0.8856. A second validation strategy, called « ten-fold », is perfomed. It consists in dividing the data set into 10 sub-sets. Therefore, ten models were provided, where each one is trained using 9 sub-sets and tested using the tenth one. The second strategy offers average accuracy equal to 0.9545, the average sensitivity is equal to 0.9643 and the average specificity reaches 0.9375.

In [68], an automated screening system based on DL is proposed to classify fundus auto-fluorescene (FAF) images into normal or atrophic AMD which is an extension of a previous version described in [75]. The proposed screening system is based onthe residual network (ResNet) composed by 50 layers. The training was performed using the cross-entropy loss function ant the « root mean square back propagation » optimizer. The training is runed using a private dataset composed by 400 images, validated using 40 images and tested using 200fundus images which are equitably partitioned into normal and atropic AMD.A transfert learning is employed where the used model is already pre-trained on the ImageNet database.The data set is augmented through radon tanformations such as flipping, zooming, rotation and translation. The screening system provides an accuracy of 0.98, a sensitivity of 0.95 and 1 for specificity.

The work described in [69] allows classifing the fundus image into no/early stage AMD or intermediate/advanced AMD stage through a DL model. The method aims to compare the performance of the proposed DL compared to a diagnosis of clinicians. Then, it compares the performance between 2 DL approaches. In this context, a first model based on AlexNet model is proposed. The initial learning rate is equal to 0.001. The training is run until achieving 50 epochs where no accuracy improvement is deduced. Then, a second model was proposed which reuse the pretrained OverFeat model as a feature extractor. This work used the Age-Related Eye Disease Study (AREDS) dataset which is composed by 130000 color fundus images from 4613 patients.All fundus images are preprocessed by detecting the retina and resizing with respect to the required input size of both DL models.

The evaluation is performed using 5-fold crossvalidation for both models, where accuracies between 88.4% and 91.6% and between 82.4and 83.9% are registred for both first and second models respectively. The obtained performance results allow deducing that second model offers a detection performance similar to the human ones.

In [70], a screening method is proposed to detect AMD from fundus images at the very early stage. The method is based on multiple instance learning framework. First, the fovea is detected in order to cropping the macula region. Then, the layers are trained iteratively untill deducing that accuracy stops increasing, the positive detection stops changing, or exceeding a training time threshold. The authors evaluate the same approach using three different models that are VGG16, ResNet50 and InceptionV3, where the VGG16 is chosen since it offers the better performing detection.

The work of [111] proposed a DL-based to classify the fundus image into early, intermediate or advanced stages. The images are cropped into square and then resized to 231x231. The method employs pre-trained ImageNet DCNN model which is composed by 19 layers followed by a linear SVM to provide classification. The evaluation is ensured using 5600 fundus images from the AREDS dataset where accuracies of 92-95%, specificities of 89.8-95.6% and sensitivity of 90.9-96.4% are registered. This study was extended in [112] where detection are evaluated for 2-class, 3-class and 4-class classifications and compared to physician grading.Knowing that VGG16 model requires a 224*224 images, the authors choose to cropping a square region where the border size is equal to 801 that corresponds to 2 times the optic discdiameter. Then, the ROI is reduced to 224*224. The dataset is composed by 3596 AMD images and 1129 healthy images. All images are acquired using Canon CR-Dgi fundus camera that provides retinal images with a resolution of 3072 × 2048.The experimental results indicate that the cropping allows achieving better result than directly extracting region of 224*224 from the fundus image, where a final average AUC about 0.79 is achieved.

In [71], the authors propose a DL model called Retinet, that classifies the fundus image into normal, dry AMD, wet AMD and others DR classes. The arcitecture is based on AlexNet which is composed by 5 convolutional layers that applies 3*3 filter followed by Rectified Linear Unit (ReLU).

RetiNet was trained using stochastic gradient descent, a momentum equal to 0.9 and a weight decay of 0.00005.All input images were preprocessed in order to reduce noising, increasing contrast and illumination. Therefore, each image is resized to 512x512. Then, several data augmentation techniques are employed which are rotation, cropping, zooming and color perturbation. The dataset integrates 62578 fundus images where 197 ones are on the Wet and Dry AMD stage which are selected from the UCH-AMD private database; the remaining fundus image are selected from Messidor and Kaggle databases. Theachieved prediction rate is about 88% and all AMD images was correctly detected.

In [72], two AMD detection DL models are proposed which offer a 4-class and a 9-class classifications, respectively. The first model affects the fundus images as no AMD, early AMD, intermediate AMD, and advanced AMD.For the second model, sixsteps correspond to different drusen area scales. Five steps correspond to pigmentary abnormality, where steps are overlapped. The authors assume that such classification allowsproviding predictive variables for 5-year risk of late AMD. The method based on the ResNet-50 network is trained and evaluaded using a private dataset fundus images. The fundus images were selected from the AREDS dataset and were divided into train, validate, and test subset which correspond respectivelly to 88%, 2%, and 10% from the whole dataset. The 4-step classification model was trained using 67401 fundus images which achieves an accuracy of 75.7% comparable to that of the ophthalmologist where accuracy is equal to 73.8%. In addition, the authors analyse the false positive results where the largest percentage error corresponds to classify the second AMD grade as first AMD grade for both human and machine (46.8%) and (34.2%) of images, respectively. The 9-step model was trained using 58370 fundus images which does not offer acceptable results, where several adjacent misclassifications were registred.

The work described in [73] uses a DL model called « DeepSeeNet », to classify fundus images into 5 severity AMD scales. The particularity of this method consists in taking into account both eyes in screening AMD. The proposed DeepSeeNet-based method ensures detecting the AMD risk factors is detected and then computing the AMD severity. In order to do this, The DeepSeeNet model is composed by 3 DL models that are performed sequentially.

A first DL model called Drusen-Net (D-Net), which detects drusen in 3 size categories (small/none, medium, and large). Then, Pigment-Net (P-Net) is the second DL model that detects the absence or presence of pigmentary abnormalities. The LA-Net (Late AMD-Net) is the last used model that detects the presence or absence of late AMD (i.e. dry or wet AMD). The three DL models correspond to an Inception-v3 architecture. The macula is defined and extracted on squaring imagesfrom all funfus images of the AREDS dataset and then scaled to 224 * 224 pixels. The training is performed using the Adam optimizer with a learning rate of 0.0001, until accuracy values was not increased in the last 5 epochs. Experiment results show that the proposed model achieves an accuracy of0.671and a kappa of 0.558where retinal specialists classify images with accuracy of0.599 and a kappa of 0.467.

In [74], the authors propose a system of 13 AMD classes based on the AREDS 9-step severity scale. The first grade indicates fundus images with little or no AMD-related changes. From second to ninth grades, fundus image present changes associated with early to intermediate AMD. Grades 10 and 11 correspond repsectivelly to Geographic atrophy and neovascularAMD,where grade 12 indicates suffering from both Geographic atrophy and noevascularisation forms. The last stage indicates that fundus image is not suitable for this proposed grading. Firstly, fundus image colors are balanced using a Gaussian filtering. Then, multiple (CNNs) are independently trained such as respectivelly AlexNet, GoogLeNet, VGG Inception-V3, ResNet and Inception-ResNet-V2. Each model is trained for 10 epochs using theloss function intitled “Cohen’s quadratic weighted k”, and then at least another 30 epochs with the “custom weighted k” loss function. The experimentation is processed using the AREDS datast where each image was scaled to 512 * 512 pixels. Then, several data augmentations are employed such as flipping, rotating and adjusting. Accuracies of all trained models are between 58.3 and 63.3. Thereafter, the results of all models are provided to a random forest algorithm that is trained using 1000 trees. The average balanced accuracy over all classes are between 70.3 and 74.7.

The work described in [68] proposes a DL-based automated system to segment the atrophic AMD using the U-Net model. Each pixel of input fundus image ismarked as non-atrophy, atrophic AMD, or other pathologies. For the training process, the Adam optimizer is used and the sigmoid cross-entropy loss is employed as loss function.

The evaluation consists at computing the DICE similarity coefficient (DSC) and the OR between AUTomatic (AUT) and MaNuaL (MNL) segmentation where equation are indicated as follows in equations 1 and 2.

$$DSC(AUT, MNL) = 2(AUT \cap MNL) / (AUT + MNL) \quad (1)$$

$$OR (AUT , MNL) = (AUT \cap MNL) / (AUT \cup MNL) \quad (2)$$

Where the provided DSC is equal to 0.94 ± 0.04, the OR is equal to $0.89 \pm 0.06$and the area difference ratio is 0.07 ± 0.31.

2.3. Diabetic Retinopathy

2.3.1. Methods and Materials

DR is one of the leading diseases of visual impairments which is one of the complications of diabetes [1]. DR is a microvascular complication of diabetes, providing morphological changes and abnormalities in the fundus. These changes concern mainly the microaneurysms (MAs), exudates (EXs, Hard and Soft Exudates), blood vessels such as the abnormal growth of the blood vessels, hemorrhages (HMs), macula interretinal micro vascular abnormalities (IRMA). The appearance of MAs and hard exudates are the earlier signs of DR. DR is a 5-point scale. The scale one is no apparent retinopathy, mild nonproliferative DR (NPDR) is the second one, and moderate NPDR, severe NPDR, and proliferative DR (PDR) are third, fourth and fifth scale respectively. PDR occurs when the new abnormal vascular blood vessels appear in different regions of fundus. Thus, in terms of classification we have five-stage disease severity for DR. Three stages involve the low risk. The fourth stage corresponds to a severe nonproliferative retinopathy. The fifth one defines a proliferative retinopathy stage. Figure 10 shows retinal image with some DR features like NPDR stage (figure 10 left) and moderate NPDR stage (figure 10 right).

Modified Davis grading [76] including Simple, Pre-Proliferate DR and PDR is also used in some works for DR classification.

In the modified Davis grading, SDR is characterized by a variety of clinical structures of retina such as microaneurysm, retinal hemorrhage, hard exudates, retinal edema and more than three small soft exudates. This set of clinical structures may include PPDR soft exudates, varicose veins, intraretinal microvascular abnormality, non-perfusion area over one-disc area, PDR neovascularization, pre-retinal hemorrhage, vitreous hemorrhage, fibro vascular proliferative membrane and tractional retinal detachment (TRD). The TRD is the second most common type of retinal detachment after a Rhegmatogenous retinal detachment (RRD).

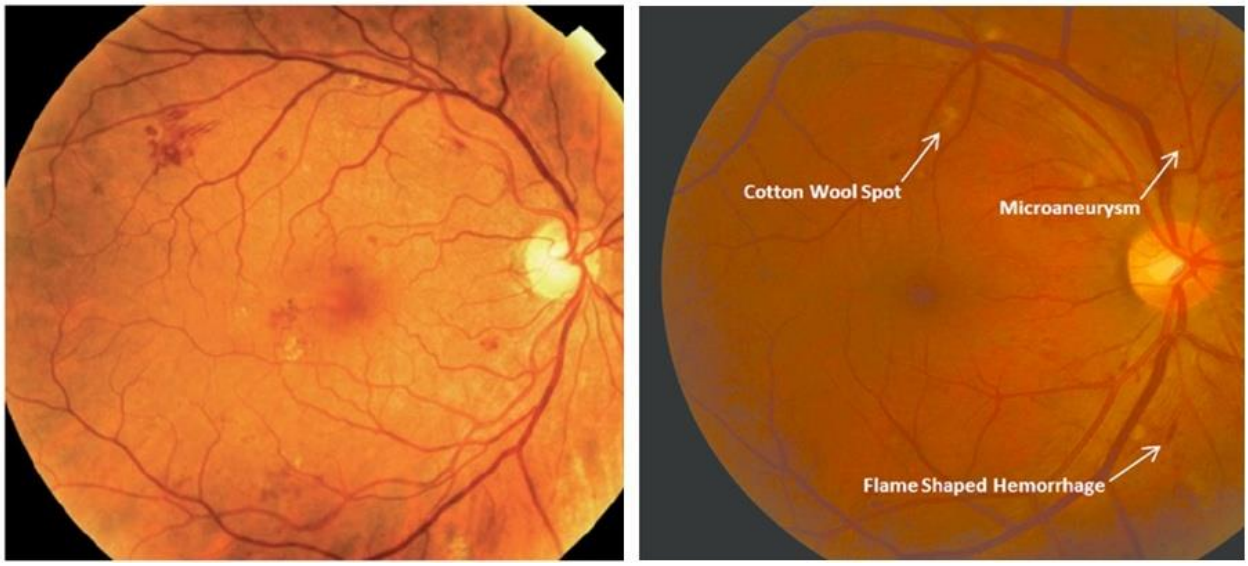

Figure 10. Retinal image with some DR features: Mild-non-proliferative diabetic retinopathy (left) and moderate non-proliferative diabetic retinopathy (right).

DR is a progressive disease and needs its detection at an early stage because it is fundamental to prevent the development of DR disease. Similarly, saving a patient's vision requires regular screening which generates developing efficient and reliable frameworks of computer assisted diagnosis of DR as CAD system. The DR diagnosis identified by the detection of abnormal structures in fundus in particular EXs, MAs, HMs, Cotton Wool Spots, bright and dark lesions. Thus, it is important to segment accurately these components for better localization, detection and identification.

Supervised and Unsupervised learning techniques are the major methods used the detection of the main clinical components of DR Disease providing automated screening based on retinal images.

These techniques of feature extraction for clustering and classification require a following preprocessing stage involving different steps such as contrast adjustment, average filtering, adaptive histogram equalization, median filtering, etc.

Recently, there are some works for DR diagnosis at image level based on DL. The comparative study of performances between DL methods and previous traditional methods shows that DL approaches achieve significantly better performance.

2.3.2. Deep-Learning based methods for DR detection and grading

Harry Pratt et al. [77] described a method based upon a network with CNN architecture and data augmentation. The proposed method can identify the main features of DR disease like micro-aneurysms, exudates and hemorrhages. The classification provides 5 grades such as No DR, Mild DR, Moderate DR, Severe DR and Proliferative DR. Data augmentation was used throughout training to improve its localisation ability. The CNN was initialized with Gaussian initialization reducing the initial training time. The proposed uses a cross-entropy function as loss function. The final trained CNN network trained on Kaggle dataset achieved 75%, 95% and 30% for accuracy, specificity and sensitivity respectively.

In [78] the proposed deep learning method aims localization of the discriminative and visual interpretable feature of DR. This method is achieved by adding the regression activation map (RAM) of an input image. The RAM concept is inspired by [79]. Two CNN networks were proposed, Net-5 and Net-4 that have different units of convolutional (Conv) and pooling (MaxPool) layers and each layer has different filters, strides and size. A global averaging pooling (GAP) layer is used to connect the last convolutional layer and the output layer. As data augmentation, image transformations are used like flipping, rotation, translation, stretching, and color augmentation. For initialization and pre-training, the orthogonal initialisation is used to initialize weights and biases. For both Net-4 and Net-5 stetting and without feature blending, the achieved Kappa scores is around 0.70 for 256 pixel images, 0.80 for 512 pixel images and 0.81 for 768 pixel images from the Kaggle dataset.

In [80] a modified fully randomly initialized GoogLeNet deep learning neural network is proposed. The modified GoogLeNet deep convolutional neural network was trained with 9443, 45° posterior pole color fundus photographs using manual modified Davis grading. The PABAK to modified Davis grading was 0.64 and accuracy is equal to 81%. The PABAK to real prognosis grading was 0.37 and accuracy is equal to 96%). One of the benefits of the proposed method is that currently useless single-field fundus photographs. This method can be used for disease staging of DR retinopathy and screening of fundus photographs.

In [81] a DCNN approach is proposes explored for the automatic classification of DR disease from color fundus image. Data augmentation is applied to artificially enlarge the used datasets including some transformation like rotation from 0° to 360°, randomly shearing with angle between -15° and 15), flipping, rescaling with scale factor between 1/1.6 and 1.6) and translation with shift between -10 and 10 pixels. The used CNN architecture consists of multiple layers like convolution layers (two 3x3 convolution, 32 filter, two 3x3 convolution 64 filter, two 3x3 convolution 128 filter and two 3x3 convolution 256 filter). Each two convolution layers are followed by a 2x2 max-pooling layer. To train the CNN, a dataset including 800 labeled images is used and 200 images are used to evaluate the performance of the trained CNN. The classification step uses the CNN and GBM (i.e. Gradient Boosting trees-based Machine). The experimental results indicate the following classification accuracies like 89.4% for Hard exudates, 88.7% for Red lesions, 86.2% for microaneurysmes and 79.1% for Blood vessel detection.

In [82] a new method for the explanation of DL classification models is proposed. This method is based on the distribution of scores. These scores are extracted from the last layer among the input pixels of the analyzed image. The EyePACS dataset is used (https://www.kaggle.com/c/diabetic-retinopathy-detection). The DR interpretable classifier is designed by applying the proposed model. The obtained results reach more than 90% of sensitivity and specificity thus providing the detection of more severe cases of Diabetic Retinopathy. The proposed model aims to classify DR disease into the five severity levels. This method gives for every class, other characteristics such as the score importance pixel maps, allowing ophthalmologists the possibility of both diagnosis deduction and interpreting the results of the classification.

The proposed model requires a reduced number of model parameters enables involving the also use of this model in low resources devices, like Smartphones.

In [83] an automated DR identification and grading system (DeepDR) detects the presence and severity of DR from fundus images via transfer learning and ensemble learning. A preprocessing step is applied to remove the invalid areas of black space, to downsize all images to a uniform size in accordance with the input requirements of specific models and to improve local contrast and enhance edge definition in each image region. For this purpose, histogram equalization (HE) and adaptive HE are used. The proposed CNN architecture includes a feature extractor and classifier. Feature extractor is based on a pre-training model that was initialized via transfer learning. The classifier made predictions on the extracted features. For a feature extractor part ResNet50 and InceptionV3, and DenseNets are used aiming to reduce gradient disappearance. The classifier is designed as customized standard deep neural network (SDNN). The first layer of the SDNN is a Goal Average Poling (GAP) laye. The second one is a fully connected layer and contains 2048 hidden neurons. To achieve the nonlinearity in the SDNN, ReLU layers are applied to the output of all inner fully connected layers, except the output layer. Kappa, Precision, Sensivity, receiver operating characteristic curve with AUC, F1-score and Youden's index (Youden's index = Sensitivity + Specificity - 1) are used as metrics to evaluate the performance of the evaluation of the proposed DL based CNN Network. Kappa > 0.8 indicates excellent consistency. The proposed identification model performed with a sensitivity of 97.5%, a specificity of 97.7% and an accuracy of 97.7%. The grading model achieved sensitivity of 98.1%, a specificity of 98.9% and an accuracy of 96.5%.

In [84] a hybrid method for diagnosing DR is proposed including both image processing and DL approach. Image processing algorithms such as histogram equalization and the contrast limited adaptive histogram equalization were applied to enhance the image quality. The DR diagnosis is performed by the classification based on DL and CNN. The MESSIDOR dataset is used and the obtained performance measures are 97% for accuracy, 94% for sensitivity, 98% for specificity 98%, 94% for precision, 94% for FScore and 95% for Geometric Mean.

In [85] DL method is presented and the image set collected and graded. The DL method was trained using the Inception version 4 model architecture and a large dataset of more than 1.6 million retinal fundus images, then tuned on a set of 2000 images that had adjudicated labels agreed on by 3 retina specialists as a reference standard. A comparison of the DR disease distribution determined by the retina specialist panel (reference standard) and the algorithm's grading shows approximately 23% of the images showed mild or worse NPDR according to the reference standard. Overall, the model showed a 5-class accuracy of 88.4%, with an accuracy of 96.9% for images with no DR and 57.9% for images with mild or worse NPDR.

In [86] the proposed framework based upon CNN network using VGGnet model have been trained with back propagation NN, Deep Neural Network (DNN) and Convolutional Neural Network (CNN). This framework seeks to identify the key antecedents of DR and is able to quantify the main features including, in addition fluid drip into different classes. This framework includes the following steps: Extracted the statistical features such average, median, standard deviation, skewness, root mean square error, mean absolute deviation quartiles, minimum, maximum and threshold level (step 1). Step 2 as preprocessing one includes resizing, median filter, morphological processing, edge detection for feature extraction and binary image conversion. To tackle some feature loss during the resizing or filtering, a Fuzzy C-Means function is applied. A statistical data processing with Feed Forward Neural Network as step 3 and image classification with FNN (Forward Neural Network and DNN (Deep Neural Network models, performing CNN based on VGG16 model as step 4 and step 5 respectively. The last step (step 6) provides a comparison result taking from step 3, step 4 and step 6 as performance and accuracy with testing image set. The accuracy percentages of proposed DNN model for both training and testing are 89.6, 86.3.

In [87] a Multi-Cell Multi-Task Convolutional Neural Networks (MCNN) is proposed. This architecture is based on a Multi-Task learning strategy which predicts the label with both classification and regression. The MCNN architecture consists of Inception-Resnet-v2 module, Multi-Cell architecture module and Multi-Task Learning module. The Kaggle dataset is used to evaluate the proposed architecture. The Experimental results achieve a quadratic weighted Kappa of 0.841.

In [88] the proposed network model is based on Transfer learning on pretrained GoogLeNet and AlexNet models from ImageNet. It achieved a sensitivity of 95%. The AlexNet and GoogLeNet architectures are trained and tested as 2-ary, 3-ary and 4-ary classification models. The Transfer learning on pretrained GoogLeNet and AlexNet models from ImageNet improved peak test set accuracies to 74.5%, 68.8%, and 57.2% on 2-ary, 3-ary, and 4-ary classification models respectively. The proposed network uses convolutional layer L2 regularization to reduce model overfitting. The cross-entropy function is used to compute error loss. The Xavier method (see for example: https://www.deeplearning.ai/ai-notes/initialization/) provides the weights initialization. AlexNet, VGG16 and GoogLeNet models were trained on the binary-labeled as normal or mild vs moderate to end stage. Kaggle dataset is used to evaluate the performance of the proposed CNNs. The GoogLeNet model is more efficient and achieved a sensitivity of 95% and specificity of 96%. The sensitivity of the no DR and severe DR classes were 98% and 93% respectively. However, the sensitivity for the mild class was only 7%. The 3-ary classifier gives sensitivities for no DR and severe DR of 85% and 75% respectively and 29% for mild class sensitivity.

In [89] a DR interpretable image classification model was described. This model is used for grading the level of the DR. The EyePACS dataset is used to get a training set which is composed of 35,126 images and the test set 53,576. The QWK metric [25] was close to the reported by human experts. The test set uses a unique DL model without ensembling. A Receptive field (RF is widespread model of sensory neurons describing the best-fitting linear transformation from the stimulus to the neural response) score distribution model is proposed. RF distributes the output score into the previous layers. The proposed CNN has 391,325 parameters, dispatched in 17 layers. The feature extractor is the first of layers and the classifier is the second group. The feature extraction has 7 blocks of 2 layers. Every layer is a stack of a 3 × 3 convolution with stride 1 ×1 and padding 1 × 1. Every layer is followed by batch normalization and a ReLU activation function. A 2 × 2 max-pooling operation of stride 2 ×2 is applied between every block. After the 7 blocks of feature extraction, the RF of the network has grown till reaching 637 ×637, corresponding approximately to the input size. The classification phase uses a 2 ×2 convolution. To get a final 64 feature, a 4 ×4 average-pooling is used to reduce the dimensionality vector. These features are linearly combined and the output scores of every class are obtained.

A SoftMax function allows the conversion of scores to probabilities. The feature extractor has 16 filters in the first block. The second block has 32 filters. The other blocks include 64 filters. The model is trained for 300 epochs. The QWK value are reached 0.814 on the validation set and 0.801 on the testing set. The testing set contains 10.000 images. A linear classifier is used to combine the features of both eyes. Using the Messidor-2 dataset, the obtained prediction performance is 91.1% and 90.8% for sensitivity and specificity respectively. The used model has 391. 325 model parameters and 17 for model depth. A proposed DR interpretable classifier, achieved more than 90% of sensitivity and specificity and allow it to detect more severe cases of DR disease.

2.3. 3. Dataset used DR diagnosis

The publicly available datasets used are Kaggle dataset, DRIVE dataset, STARE dataset, EyePACS dataset and MESSIDOR dataset.

In [83] macula-centred retinal fundus images were taken from the Sichuan Academy of Medical Sciences and Sichuan Provincial Peoples Hospital. The original data comprising 13.767 images of 1872 patients were collected from three sources: ophthalmology, endocrinology and physical examination centres view were captured per eye.

In [86] the data sets we have used are FUNDUS images of human retina having pixels over 2000×3000. The dataset downloaded from website kaggle.com, dataset having over 35000 images for training and 15000 images for testing.

In [87] the dataset used is Kaggle. The retinal images were provided by EyePACS, which is a free platform for retinopathy screening. The dataset consists of 35126 training images, 10906 validate images and 42670 test images.

In [88] Experimental studies were conducted using two primary datasets. The Kaggle dataset contains 35,000 retinal images with 5-class labels such as normal, mild, moderate, severe, end stage.

The second used dataset is Messidor-1 dataset that has 1,200 color fundus images with 4-class labels. In addition, two fundoscope image datasets are used to train an automated classifier for this study.

2.4 Cataract

2.4.1 Methods and Materials

The lens allows light access to the retina to intercept signals. It is contoured by ciliary muscles that adjust eye focus in order to ensure clear vision. The protein decrease in the lens leads to clouding its texture. Therefore, the light is disrupted and hence not be projected adequately on the retina, which leads to a blurred vision, as indicated in Figure.11. b. Cataract appears often for elderly people. Aside aging, the principal factors include smoking, poor health habits, prolonged exposure to sunlight, diabetes and alcohol.

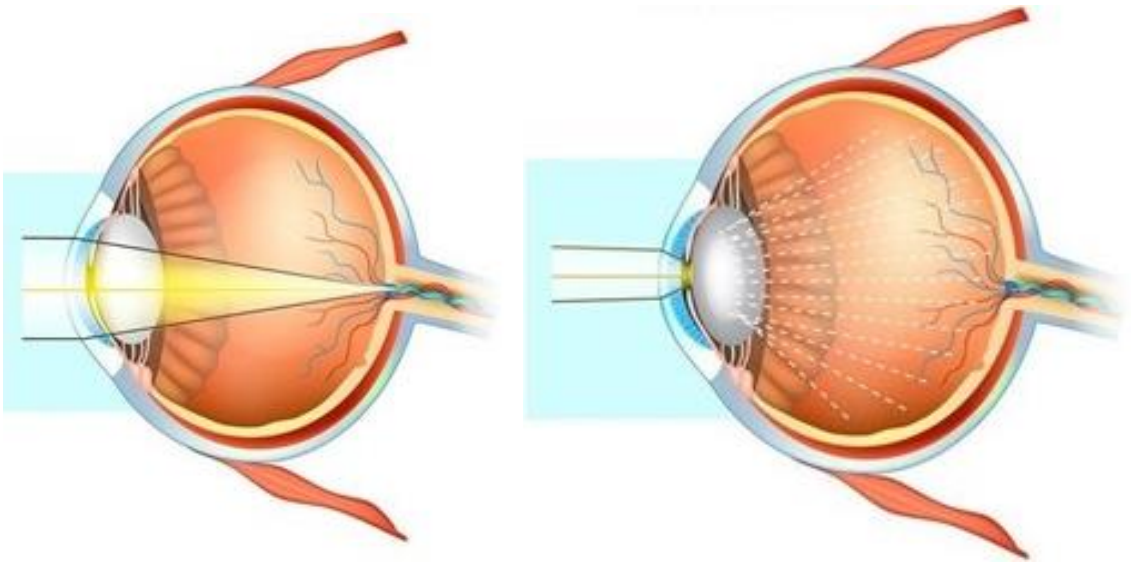

(a) (b)

Figure 11. (a) Healthy eye; (b) eye suffering of cataract [113]

Cataract might lead to blindness which is the main cause among ocular pathologies [92], with a ratio about 51% [90]. Blind people due to cataracts are about 20 million, and will exceed 40 million by 2025, based on World Health Organization report.

A cataract progress slowly which can achieve higher severity that requires surgical treatments [91], [92].

The cataract is graded to four classes: healthy, Mild, Moderate and Severe. Mild class can be treated through enhancing health habits, stop smoking and using wearing sunglasses. Therefore, early detection is higher recommended to assist patients. However, lack of ophthalmologists avoids ensure periodic diagnosis [91]. The cataract can be detected through four main methods that are light-focus method, iris image projection, slit lamp examination and transillumination ophthalmoscopy [92]. Those methods are costly and time-consuming. Therefore, this develops the necessity to propose a computer-aided diagnosis for cataract detection [90]. In this context, several automated methods are proposed which aim to detect cataract from fundus image. In the case of healthy retina, all retinal structures can be well distinguished such as optic disc and thick and thin vessels. In the case of mild cataract, thin vessels are slightly visible. However, only thick vessels and optic disc are visible in the moderate stage. In the last stage, no retinal structures can be seen [91, 92]. Figure 12 shows (b) fundus image in mild cataract stage (figure 12.b), fundus image in moderate cataract stage (figure 12.c) and fundus image in severe cataract stage (figure 12.d).

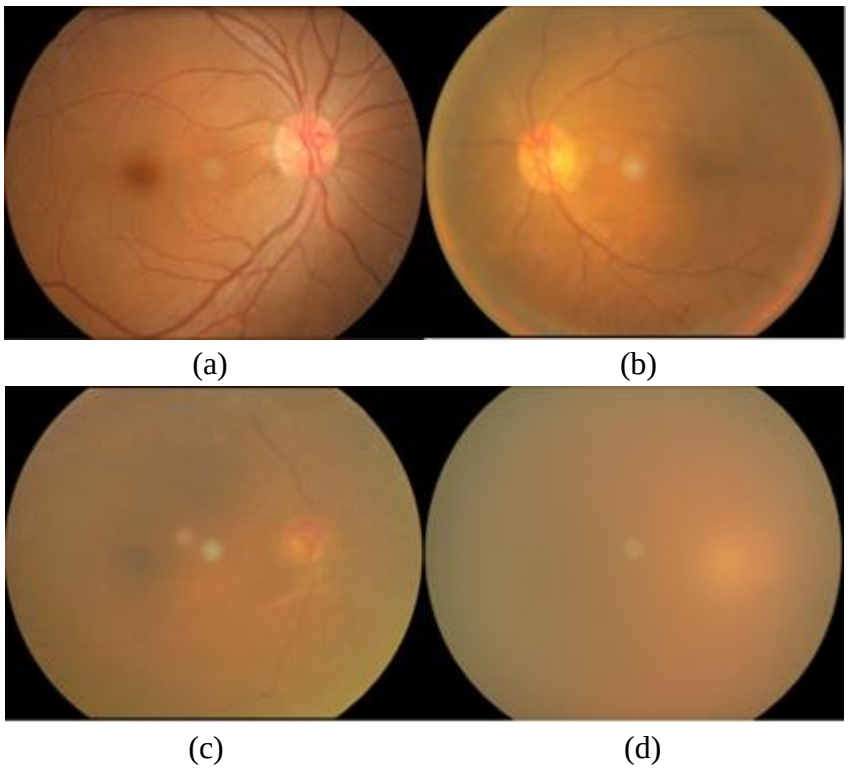

Figure 12. (a) healthy fundus image; (b) fundus image in mild cataract stage; (c) fundus image in moderate cataract stage; (d) fundus image in severe cataract stage [92]

2.4.2 Deep-Learning based methods for Cataract detection and grading

The method proposed in [92] offers an automated method for cataract detection and grading using DCNN. The fundus images are resized uniformly, and the uneven illumination is eliminating, and the green channels are extracted. Thereafter, the method employed a DCNN with five convolutional layers; three are fully connected layers and a four-way SoftMax which provide the fundus image cataract grading. A private dataset is used which is composed by 3269 images without cataract disease and 2351 healthy ones, which regarded into 4 classes. The proposed method achieves an accuracy of 93.52% to detect the cataract and an accuracy of 86.69% for providing the cataract stage grading.

In [90], the authors propose a computer-aided automatic method for cataract detection where fundus images are classified into four stages which normal, mild, moderate, and severe. After extracting the green channel, only fundus images with a good quality are conserved. This step is performed using the Naturalness Image Quality Evaluator (NIQE) and the Perception based Image Quality Evaluator (PIQE) that generates a score related to the image quality. The fundus images where scores surpass a specific threshold are taking into account. Thereafter, the features are extracted using Alex Net model which is pre-trained using ImageNet database. This model is composed by five convolutional layers followed by three fully connected layers. The features are provided to a classifier that is determinate experimentally. The authors proceed to compare several classifiers which are linear SVM, kernel SVM, K-nearest neighbour, Naive Bayes, decision tree, LDA and SoftMax, where linear SVM allows achieving the higher classification accuracy.

The dataset is collected from several public such as HRF, STARE, DIARETDB0, E-opt, MESSIDOR, DRIVE and DRIONS-DB, where 200 fundus images are chosen for each cataract grade. Based on experimental result, the method achieves an accuracy of 100% when used for two class (normal vs. cataract) classification. In the case of Four class classification, an average accuracy of 92.91 % is achieved and accuracy per stage are respectivelly100% for normal, 93.33% for middle, 88.33% for moderate, 90% for severe cataract. The experiment shows each misclassification consists in grading the image as neighborhood cataract classes.

The work described in [93] and [94] propose an automated system for grading the severity of nuclear cataracts based on convolutional-recursive neural networks (CRNN). First, the lens structure is partitioned into anterior cortex, nucleus, and posterior cortex. Thereafter, the three sections are resized where anterior cortex and posterior cortex are scaled in square shapes, where width is the half of the nucleus one. The resizing is done while preserving the same lens structure dimension. Then, anterior section is removed, and the nucleus is divided into three overlapped sections. Afterwards, the grading category is used to learn local features from each section. Thereafter, local patches from each section are randomly extracted and merged into the same group. Those features are provided to a convolutional layer of the CNN. Hence, image contrasts are normalized, and average pooling is applied. Then, N random RNNs are performed to extract N vectors of higher order features. Finally, those vectors are injected into support vector regression (SVR) to provide the final grading result. This method is evaluated using the ACHIKO-NC dataset that contains 5378 images. Each image is graduated from 0.1 to 5.0, which is defined using the Wisconsin protocol. Four metrics are computed to evaluate the method that are the integral agreement ratio (R_0), the ratio of decimal grading errors$\leq$ 0.5 ($R_{e0.5}$), the ratio of integral grading errors$\leq$ 1.0($R_{e1.0}$), and the mean absolute error (ε), which values are respectively 0.704 ±0.016, 0.881 ±0.019, 0.990 ±0.004 and 0.307 ±0.019.

In [91], a grading cataract severity method of fundus image is proposed. The method models the four-class classification problem into three adjacent two-class classification problems. After delimiting the retina, an improved version of the “Haar wavelet filter” is applied to the fundus image in order to decompose it into Approximate Components (ACs). Those ACs should be classified through three optimal thresholds that correspond to the three two-class classifiers. The authors proposed to define them through on « mean square error » loss function of the BP-net model, where those values are generated when DL model provides a higher accuracy classification. The evaluation is performed using a private dataset composed by 1355 retinal images. The experiment shows that two-class classification and four-class classification achieve respectively accuracies about 94.83% and 85.98%.

3. Deep Learning-bases Smartphone for detection of retinal abnormalities

3.1 Smartphone Captured fundus image evaluation

Nowadays, the design of the CAD-based Smartphone for detection of retina abnormalities is growing. Several works are interested to the quality of fundus image captured by Smartphone, with respect to the clinical employment. The work described in [95] describes an experimentation that evaluates the D-EYE lens captured fundus images with respect to the direct ophthalmoscope ones.

In [96], ophthalmologists deduced that Smartphone captured fundus images are readable with an average between 86% and 100%, and have an accepted quality in 93%-100%.

Jin et al. [97] were summarized a qualitative comparison study between portable and tabletop fundus camera by grading 400 fundus images in each category. The ophthalmologists assign excellent overall quality about 63% and 70.75% and inadequate quality about 4.75% and 3.25% respectively for portable and tabletop camera.

They are some based-Smartphone camera devices with non-mydriatic camera, as for examples: PEEK Retina (Peek Vision, London), D-Eye (D-Eye; Pasadena, Calif. with undiluted pupils, a field of view of 5-8º, and the optic disc detection with pupils as small as 2mm), HFC MicroClear is handled-portable with 45° field view, the ZEISS VISUSCOUT 100 - Handheld Fundus Camera has a non-mydriatic operation, with color and red-free images and 40° field of view. Figure 13 shows some Non-mydriatic and portable fundus camera devices.

Figure 13. Some Non-mydriatic and portable fundus camera devices: a) Horus DEC 200 Hand Held Fundus Camera (https://www.bibonline.co.uk/) with 40° manual focus portable fundus camera); b) ZEISS VISUSCOUT 100 - Handheld Fundus Camera (https://www.zeiss.com/); c) Volk iNview -iPhone Fundus Camera (https://www.foresightintl.com/) and d) The D-EYE Retinal Camera (https://www.d-eyecare.com/).

Other works have been proposed for screening and diagnosis of ocular diseases. In [98] a screening tool is given. This tool is able to identify patients with Diabetic Retinopathy. The D.EYE device is used.

Russo et al. [99] aim to calculate the Vertical Cup-to-Disc Ratio value. For the experimental results, a Smartphone ophthalmoscopy equipped with D-EYE lens and slit-lamp biomicroscopy were used and the obtained Kappa is equal to 0.63.

Thomas et al. [100] propose a Tele-glaucoma providing a specificity of 79% and a sensibility of 83%.

In [101] the DR detection uses Smartphone fundus photography. This work shows that both non-mydriatic fundus photography and Smartphone are able to detect DR. The non-mydriatic one is more sensitive.

A. Elloumi et al. [102] and [103] propose a Smartphone based method for Optic Nerve Head detection from fundus images captured by the D. EYE lens. The STARE and DRIVE databases are used and the obtained results are 96% and 100% detection rates on STARE and DRIVE Datasets respectively.

The average execution times are 2s on STARE dataset and 1.3s on DRIVE database. The proposed image processing pipeline in order to detect and enhance the retina area and detect the Optic Nerve Head in Smartphone less than 1 second.

The table 1 shows the characteristics and performance of ocular diseases detection using from Smartphone and fundus image that we have identified in some related works.

Table 1. *Some related work based-Smartphone for ocular disease detection*

Works	**Pathologies**	**Fundus image number**	**Performance - Evaluation**	**Capture device**
Toy et al [98]	moderate non-proliferative &Worse diabetic retinopathy	100	91% sensitivity 99% specificity 95% positive predictive value 98% negative predictive value.	Paxos Scope
Russo et al. [99]	Vertical Cup-to-Disc Ratio (glaucoma)	107 s	95% sensitivity 95% specificity 63 % Kappa (k)	D-EYE
Rajalakshmi et al. [104]	DR	---	92.7 % sensitivity 98.4 % specificity Kappa (κ) = 0.90	(FOP) camera
Muiesan et al. [105]	hemorrages exudates papiledema	104	Hemorrages: 0.795 Exudates: 0.822 – 0.878 Papiledema: 0.815 – 0.804	D-Eye
Thomas et al. [100]	Glaucoma	---	83% sensitivity 79% specificity	

3.2 Deep-Learning based method of ocular pathology detection from Smartphone-captured fundus image

It is only recently that an interest is focused on the design of CAD systems based on DL and using Smartphone for detection of retinal abnormalities. However, there is very little published work. The following works [106, 107, 108] illustrate using DL on Smartphone for screening and diagnosis of ocular pathologies.

Uncorrected Refractive Error (URE) is one of the most important consequences of visual impairment. In [106] a method based on DL is proposed to extract information, such as URE from fundus.

Figure14 presents an overview of the proposed Deep neural network. The used retinal fundus images were 45° and 30° field of view images from the UK Biobank (http://www.ukbiobankeyeconsortium.org.uk/) and AREDS. The proposed DL algorithm is trained to predict URE error from a total of 226.870 images. The validation was done on 24.007 UK Biobank and 15.750 AREDS images. As cited in [106], the obtained results have a mean absolute error of 0.56 diopters (95% Confidence Interval (CI): 0.55–0.56) for estimating spherical equivalent on the UK Biobank dataset and 0.91 diopters (95% CI: 0.89–0.93) for the AREDS data set. The baseline expected mean absolute error obtained by simply predicting the mean of this population was 1.81 diopters (95% CI: 1.79–1.84) for UK Biobank and 1.63 (95% CI: 1.60–1.67) for AREDS. The proposed Deep Neural network is consistent with the implementation on portable devices, such as Smartphone equipped with portable fundus camera [109] and may also be used to measure the visual acuity [110]. The authors were also considering his use as a Smartphone application of screening and diagnosing ocular disease in the developing world.

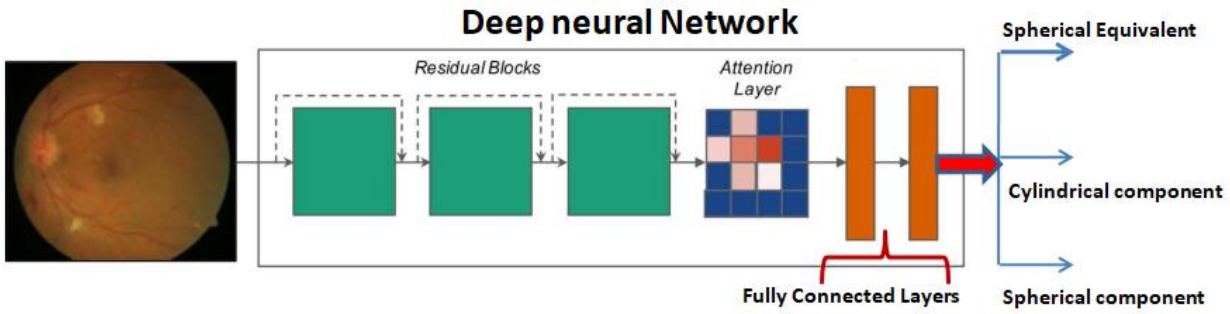

Figure 14. Overall framework of the proposed Deep neural network model in [106].

In [107] the authors propose artificial intelligence (AI)-based automated software for detection of DR and Sight-Threatening DR (STDR) from fundus photography. The images are captured by a Smartphone-based device. STDR was defined by the presence of severe non-proliferative DR, proliferative DR or diabetic macular oedema (DME). DR screening software EyeArt TM (version v2.1.0) is used for grading the retinal photographs.

The EyeArt AI algorithm has been clinically trained and validated using retinal images of 78,685 patients. The retinal images were taken by conventional desktop mydriatic fundus cameras (http://www.eyepacs.com/data-analysis). The obtained results were based on retinal images of 296 patients that are graded. DR was detected by the ophthalmologists in 191 (64.5%) and by the AI software in 203 (68.6%) patients while STDR was detected in 112 (37.8%) and 146 (49.3%) patients, respectively. The AI software showed 95.8% (95% CI 92.9–98.7) sensitivity and 80.2% (95% CI 72.6–87.8) specificity for detecting any DR and 99.1% (95% CI 95.1–99.9) sensitivity and 80.4% (95% CI 73.9–85.9) specificity in detecting STDR with a kappa agreement of $k = 0.78$ ($p < 0.001$) and $k = 0.75$ ($p < 0.001$), respectively.

The CAD system proposed in [108] uses the D. Eye lens to capture and process fundus images in real-time on Smartphone platforms for retinal abnormality detection. It is based on CNN and the transfer learning method. The transfer learning method is based on the pre-trained Exception (Extreme version of Inception) model. The pre-trained Exception model was trained using the ImageNet database (http://www.image-net.org/). A block diagramed the architecture of the Xception transfer learning used here for diabetic retinopathy detection is shown in Figure 15.

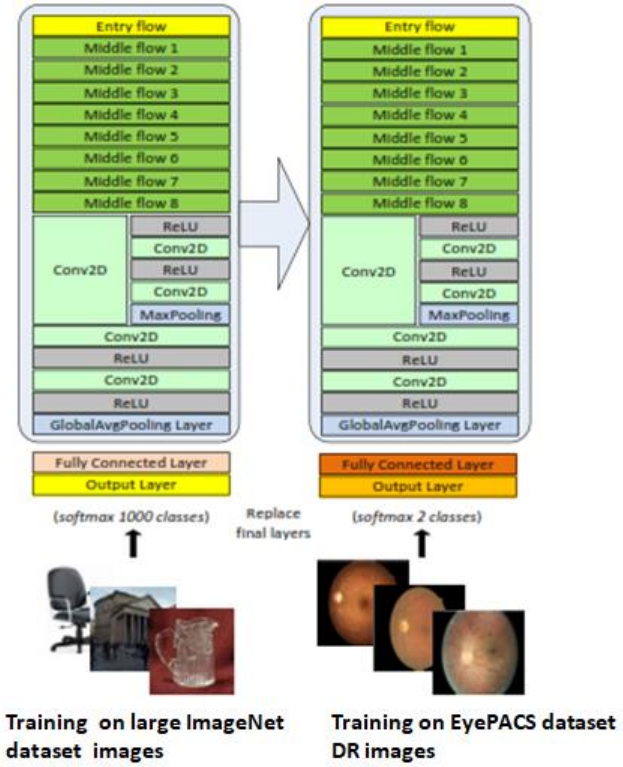

Figure 15. Transfer learning architecture used for diabetic retinopathy detection [108].

The real-time results reported in this work are based on the iPhone 7/ iPhone XR iOS Smartphone and Pixel 2/ Pixel 3Android Smartphone. In the iOS version of the developed app, 30 frames get captured per second and two detection decisions are made per second. The DR CNN model was trained and tested on the retina images from the EyePACS dataset corresponding to no diabetic retinopathy (label 0), and the severe diabetic retinopathy (labels 3 and 4). 23354 retina images were used for training and 4037 images selected at random were considered for testing. The overall accuracy of the diabetic retinopathy detection was found to be 94.6%.

4. Discussion

Glaucoma, AMD, DR and Cataract constitute the main retinal diseases. Unless early screening, these diseases lead always to severe damage on visual acuity and may be irreversible. The automated methods based on image analysis for ocular diseases diagnosis from both fundus and OCT images have been explored extensively. This category of methods is generally based on two main stages: image processing techniques (segmentation, feature extraction, and detection of retinal vessels and lesions) and ocular diseases classification and screening. Sometimes pre-processing and post-processing stages can be required. The performance evaluation of this category of methods (called in the literature “traditional methods”) is done on different public and/or private datasets, using the labels provided by experts for each fundus image of the database. Different performance metrics like accuracy (ACC), sensitivity and specificity are used to measure and evaluate the performance of the proposed methods.

Nowadays, DL and CNN have shown their abilities in different health domains including ophthalmology [16]. DL and CNN can identify, localize, quantify and analyze pathological features and ocular diseases and their performance keeps growing. In this chapter, we tried to address different kinds of applications of deep learning methodologies in ophthalmic diagnosis. So, the most severe ocular diseases are considered. Then, we focused on existing methods of earlier screening and diagnosis of these diseases.

An overview of CNN Deep Learning Networks based approaches was provided. Traditionally glaucoma is diagnosed by measuring the intraocular pressure (IOP) with a tonometer and rating an abnormal high-pressure rate. Otherwise, glaucoma can be diagnosed within the assessment of the ONH by extracting indicators such as the Cup-to-Disc Ratio (CDR) [28], the Inferior Superior Nasal Temporal (ISNT) rule [29], the RNFL thickness [30], parapapillary atrophy [31] or ONH hemorrhages [30].In the last decade, deep learning has been extensively applied for ophthalmic diagnostics achieving good results on various fundus and OCT datasets. Optic Disc, Cup and Nerve Head Segmentation is an important step for automatic cropping of the region of interest for further processing [32].

Fundus image present a mainly element to detect and grade AMD, where several DL-based methods are proposed. Based in this bibliographic study, the methods aiming for grading the fundus image into the standard 4-class classification (no AMD, early AMD, intermediate AMD, and advanced AMD) or into a reduced version of the 4-class classification (no/early vs intermediate/advanced) and achieve a higher acceptable performance detection, which can be employed in clinical context. However, works aiming for grading in large-class classification are failed to perform acceptable grading. Furthermore, we distinguish a lack of works aiming for segmenting drusens lesions where the achieved performances are not sufficient, which present a good challenge for future studies.

The appearance of microaneurysms (MAs) and hard exudates are the earlier signs of DR. In terms of classification we have five-stage disease severity for DR including three stages of low risk, a fourth stage of severe nonproliferative retinopathy, and a fifth stage of proliferative retinopathy. Recently, there are some works for DR diagnosis at image level based on DL comparing the performance between DL method and previous traditional methods and showing that DL learning achieves significantly better performance in DR diagnosis.

The cataract can be detected through four main methods that are light-focus method, iris image projection, slit lamp examination and transillumination ophthalmoscopy [92]. Those methods are costly and time-consuming. Therefore, this develops the necessity to propose a computer-aided diagnosis for cataract detection [90].

It can be noticed that in most of the cases deep learning methods outperformed traditional methodologies.

Recently, some works are interested to the quality of fundus image captured by Smartphone with respect to the clinical employment and then an interest is focused on the design of CAD systems-based DL using Smartphone for detection of retinal abnormalities. However, until now they still very little published work. In the context of ophthalmic diagnosis this can be an important direction for future research.

5. Conclusion

Throughout the study that we have carried out on part automated methods based on image analysis for eye diseases and other part deep learning-based AI in ocular diseases diagnosis, we note that there is an active effort to create and develop methods to automate screening of retinal diseases. Many CAD systems for ocular diseases have been developed and are widely used. It was also noted that the automated methods based on image analysis for ocular diseases diagnosis from both fundus and OCT images have been explored extensively.

However, the performance evaluation of this category of methods is done using a variety of public and/or private datasets. These datasets are ACHIKO-K, DRIONS-DB, HRF, SEED, ORIGA, RIGA, REFUGE (for Glaucoma), Kaggle dataset, DRIVE dataset, STARE dataset, EyePACS dataset, DIARETDB0, DIARETDB1, and MESSIDOR dataset (for DR disease), AREDS (for AMD) and other datasets such as E-ophta, MESSIDOR, DRIONS-DB. Several datasets contain fundus images where labels are provided by experts for each fundus image of the database, such as DR lesion existence in the DIARETDB0 dataset, or glaucoma disease detection in HRF dataset. However, in opposite cases, authors are required to provide labels for fundus images, where approaches are not described or not carried to ensure a performing labelling or grading.

These previous methods under-perform due to variations in image properties and quality resulting from the use of varying capture devices and the robustness and accuracy of the used approaches for ROI detection and segmentation of the retinal structures.

For all these reasons, DL and CNNs have shown their abilities in different heath domains including ophthalmology. DL and CNNs are able to identify, localize, quantify and analyze pathological features in fundus images.

We have discussed over 100 papers in CAD systems for ocular diseases that focus on the use of CNN Deep Learning Networks in detection of retinal abnormalities using retinal images.
We focused on earlier screening and diagnosis of glaucoma, age-related macular degeneration, and diabetic retinopathy and cataract diseases.

In particular, we will report the related works based on Hybrid and fully methods. The hybrid method employs both image processing for preprocessing and post processing steps and deep learning for feature segmentation and classification with CNN Deep Learning Networks. In fully method, CNN Deep Learning Networks is used for both feature extraction and classification from the input directly. Two types of retinal imaging modalities will be considered, Optical Coherence Tomography and fundus camera for capturing fundus images as inputs for the Computer-Aided Diagnosis System based upon CNN Deep Learning network.

This variety of works and methods show that we have achieved excellent reults in terms of classification and grading accuracy of ocular diseases. From this review, we can note the following works. Zhixi et al. [43] used the Inception-v3 architecture obtaining an accuracy of 98.6% Glaucoma classification. In [68], an automated screening system based on Deep Learning is proposed to classify fundus autofluorescene images into normal or atrophic age-related macular degeneration. The proposed screening system is based onthe residual network. The screening system provides an accuracy of 0.98, a sensitivity of 0.95 and 1 for specificity. In [83], an automated diabetic retinopathy identification and grading system detects the presence and severity of diabetic retinopathy from fundus images via transfer learning and ensemble learning. The proposed identification model performed with a sensitivity of 97.5%, a specificity of 97.7% and an accuracy of 97.7%. The grading model achieved sensitivity of 98.1%, a specificity of 98.9% and an accuracy of 96.5%. In [91], a grading cataract severity method of fundus image is proposed, and the experiment shows that two-class classification and four-class classification achieve respectively accuracies about 94.83% and 85.98%.

It is only very recently that an interest is focused on the design of CAD systems based upon Deep learning and using Smartphone platform for detection of retinal abnormalities. The CAD system proposed in [108] uses the D. Eye lens to capture and process fundus images in real-time on Smartphone platforms for retinal abnormality detection. It is based on convolutional neural network and the transfer learning method. The transfer learning method based on the pre-trained Exception (Extreme version of Inception) model. The pre-trained Xception model was trained using the ImageNet database. The overall accuracy of the diabetic retinopathy detection was found to be 94.6%.

References

1. Seth R Flaxman, Rupert R A Bourne, Serge Resnikoff, Peter Ackland, Tasanee Braithwaite, Maria V Cicinelli, Aditi Das, Jost B Jonas, Jill Keeffe, John H Kempen, Janet Leasher, HansLimburg, Kovin Naidoo, Konrad Pesudovs, Alex Silvester, Gretchen A Stevens, Nina Tahhan, Tien Y Wong, Hugh R Taylor. Global causes of blindness and distance vision impairment1990–2020: a systematic review and meta-analysis. Lancet Glob Health 2017; 5: e1221–34published Online October 11, 2017. http://dx.doi.org/10.1016/S2214-109X (17)30393-5

2. Bourne, R.R.; Stevens, G.A.; White, R.A.; Smith, J.L.; Flaxman, S.R.; Price, H.; Jonas, J.B.; Keffer, J.; Leasher, J.; Naidoo, K.; et al. Vision Loss Expert Group. Causes of vision loss worldwide, 1990–2010: A systematic analysis. Lancet Glob. Health 2013, 1, e339–e349.

3. Wong, T.Y.; Su, X.; Li, X.; Cheung, C.M.; Klein, R.; Cheng, C.Y.; Wong, T.Y. Global prevalence of age-related macular degeneration and disease burden projection for 2020 and 2040: A systematic review and meta-analysis. Lancet Glob. Health 2014, 2, e106–e116.

4. Jonas, J.B.; Aung, T.; Bourne, R.R.; Bron, A.M.; Ritch, R.; Panda-Jonas, S. Glaucoma. Lancet 2017, 390, 2183–2193.

5. Wong, T.Y.; Cheung, C.M.; Larsen, M.; Sharma, S.; Simo, R. Diabetic retinopathy. Global Estimates on the Number of People Blind or Visually Impaired by these major eye diseases. Nat. Rev. Dis. Primers 2016, 17, 16012.

6. Zhou Zhang, Ruchir Srivastava, Huiying Liu, Xiangyu Chen, Lixin Duan, Damon Wing Kee Wong, Chee Keong Kwoh, Tien Yin Wong, Jiang Liu. A survey on computer aided diagnosis for ocular diseases. BMC Medical Informatics and Decision Making2014, 14:80

7. Manivannan A., Kirkpatrick J. N. P., Sharp P.F., Forrester J. V. Novel approach towards colour imaging using scanning laser ophthalmoscope. Br. J. Ophthalmol. 82(4), 342-345 (1998). 10. 1135/bjo. 82.4.342.

8. Hermann B, Fernandez EJ, Unterhubner A, Sattmann H, Fercher AF, Drexler W, Prieto PM, Artal P. Adaptative-optics ultrahigh-resolution optical tomography. Opt Let 2004: 29:2142-2144.

9. Del Hoog, E., Schwiegerling, J. Fundus camera systems: a comparative analysis. Appl. Opt. 48(2): 221-228 (2009).

10. R Michael D. Abràmoff, Mona K. Garvin, Milan Sonka. Retinal Imaging and Image Analysis, IEEE Rev Biomed Eng. 2010 January 1; 3: 169–208. doi:10.1109/RBME.2010.2084567.

11. Narasimha-Iyer H, Can A, Roysam B, Stewart C, Tanenbaum H, Majerovics A, Singh H: Robust detection and classification of longitudinal changes in color retinal fundus images for monitoring diabetic retinopathy IEEE Trans Biomed Eng 2006, 53(6):1084–1098.

12. Rüdiger Bock, Jörg Meier, Georg Michelson, László G. Nyúl, Joachim Hornegger. Classifying Glaucoma with Image-Based Features from Fundus Photographs. Proceedings of the 29th DAGM conference on Pattern recognition. Pages 355-364. Heidelberg, Germany, September 12 -14, 2007.

13. A. Mvoulana, R. Kachouri, M. Akil. Fully Automated Method for Glaucoma Screening using robust Optic Nerve Head detection and unsupervised segmentation-based Cup-to-Disc Ratio computation in Retinal Fundus Images. Accepted in Computerized Medical Imaging and Graphics journal. July 2019.

14. Muthu Rama Krishnan Mokihi. Rajendra Acharyaa, Hamido Fujitad , Joel E.W. Koha, Jen Hong Tana , Chua Kuang Chuaa , Sulatha V. Bhandarye , Kevin Noronhaf , Augustinus Laudeg, Louis Tongh. Automated Detection of Age-Related Macular Degeneration using Empirical Mode Decomposition. In Knowledge-Based Systems 89:654–668· September 2015. DOI: 10.1016/j.knosys.2015.09.012

15. Huang W, Chan KL, Li H, Lim JH, Liu J, Wong TY: A computer assisted method for nuclear cataract grading from slit-lamp images using ranking. IEEE Trans Med Imaging 2011, 30(1):94–107.

16. Ursula Schmidt-Erfurth, Amir Sadeghipour, Bianca S. Gerendas, Sebastian M. Waldstein, Hrvoje Bogunovic. Artificial intelligence in retina. Progress in Retinal and Eye Research 67(2018) 1–29

17. Quigley, H. A. and Broman, A. T. (2006). The number of people with glaucoma worldwide in 2010 and 2020. British journal of ophthalmology, 90(3):262-267.

18. Costagliola, C., Dell'Omo, R., Romano, M., Zeppa, L., and Parmeggiani, F. (2009a). Pharmacotherapy of intraocular pressure: part ii. Parasympathomimetic, sympathomimetic and sympatholytics. Expert Op in Pharmacother, 10(17):2859-2870.

19. http ://www.ch-libourne.fr/offres-de-soins/pratiques-professionnelles/glaucome/

20. MT Nicolela, JR Vianna. Optic Nerve: Clinical Examination, in Pearls of Glaucoma Management. Springer, Berlin, Heidelberg. Pages 17-26, 2016.

21. Bourne, R. R. (2007). Papille optique et glaucome. Revue de Santé Oculaire Communautaire, 4(3):8-9.

22. Tham, Y.-C., Li, X., Wong, T. Y., Quigley, H. A., Aung, T., and Cheng, C.-Y. (2014). Global prevalence of glaucoma and projections of glaucomaburdenthrough2040: a systematic review and meta-analysis. Ophthalmology, 121(11):2081-2090.

23. World Health Organization, 2006. Vision 2020. The Right to Sight. Global Initiative for the Elimination of Avoidable Blindness. WHO Press

24. S Liu, SL Graham, A Schulz, M Kalloniatis, B Zangerl, W Cai, Y Gao, B Chua, H Arvind, J Grigg, et al. A deep learning-based algorithm identifies glaucomatous discs using monoscopic fundus photographs. Ophthalmology Glaucoma, 1(1):15-22, 2018.

25. Tunnel vision: the economic impact of primary open angle glaucoma.

26. Graham Mowatt; Jennifer M. Burr; Jonathan A. Cook; M. A. Rehman Siddiqui; Craig Ramsay; Cynthia Fraser; Augusto Azuara-Blanco; Jonathan J. Deeks. Screening Tests for Detecting Open-Angle Glaucoma: Systematic Review and Meta-analysis. In Investigative Ophthalmology & Visual Science, December 2008, Vol. 49, No. 12.

27. Fu, Huazhu; Xu, Yanwu; Lin, Stephen; Wong, Damon Wing Kee; Mani, Baskaran; Mahesh, Meenakshi; Aung, Tin; Liu, Jiang. Multi-Context Deep Network for Angle-Closure Glaucoma Screening in Anterior Segment OCT. Médical Image Computing and Computer Assisted Intervention (MICCAI) 2018. ArXiv :1809.03239

28. Shen, S. Y., Wong, T. Y., Foster, P. J., Loo, J.-L., Rosman, M., Loon, S.-C., Wong, W. L., Saw, S.-M., and Aung, T. (2008). The prevalence and types of glaucoma in Malay people: the Singapore Malay eye study. Investigative ophthalmology&visual science, 49(9):3846-3851.

29. Thakkar, K., Chauhan, K., Sudhalkar, A., Gulati, R., and Ophthalmologist, M. (2017). Detection of glaucoma from retinal fundus images by analysing isnt measurement and features of optic cup and blood vessels. Int. J. Eng. Technol. Sci. Res. IJETSR, 4(7):2394-3386.

30. Fingeret, M., Medeiros, F. A., Susanna Jr, R., and Weinreb, R. N. (2005). Five rules to evaluate the optic disc and retinal nerve fiber layer for glaucoma. Optometry-Journal of the American Optometric Association, 76(11):661-668.

31. Jonas, J. B., Fernandez, M. C., and Naumann, G. O. H. (1992). Glaucomatous Parapapillary Atrophy: Occurrence and Correlations. JAMA Ophthalmology, 110(2):214-222.

32. Soorya Sengupta, Amitojdeep Singh, Henry A. Leopold, Tanmay Gulati, Vasudevan Lakshminarayanan. Ophthalmic Diagnosis and Deep Learning - A Survey. Computer Vision and Pattern Recognition 1812.07101 (2018).

33. Z. Feng, J. Yang, L. Yao, Y. Qipao, Q. Yu, X. Xu. Deep retinal image segmentation: A fcn-based architecture with short and long skip connections for retinal image segmentation (2017) 713-722.

34. L. Fang, D. Cunefare, C. Wang, R. Guymer, S. Li, S. Farsiu, Automatic segmentation of nine retinal layer boundaries in oct images of non-exudative amd patients using deep learning and graph search, Biomedical optics express 8 (5) (2017) 2732-2744.

35. M. Pekala, N. Joshi, D. Freund, N. Bressler, D. DeBuc, P. Burlina, Deep learning based retinal oct segmentation, arXivpreprintarXiv:1801.09749.

36. Zilly, Julian; Buhmann, Joachim M; Mahapatra, Dwarikanath. Glaucoma detection using entropy sampling and ensemble learning for automatic optic cup and disc segmentation. Computerized Medical Imaging and Graphics 55 (2017) 28–41

37. S Liu, SL Graham, A Schulz, M Kalloniatis, B Zangerl, W Cai, Y Gao, B Chua, H Arvind, J Grigg, et al. A deep learning-based algorithm Identifies glaucomatous discs using monoscopic fundus photographs. Ophthalmology Glaucoma, 1(1):15-22, 2018.

38. X. Chen, Y. Xu, S. Yan, D. Wong, T. Wong, J. Liu, Automatic feature learning for glaucoma detection based on deep learning (Oct 2015).URL https://link.springer.com/chapter/10.1007/978-3-319-24574-4_80

39. Y. Chai, H. Liu, J. Xu, Glaucoma diagnosis based on both hidden features and domain knowledge through deep learning models. Knowledge-Based Systems. doi: 10.1016/j.knosys.2018.07.043.

40. H. Fu, J. Cheng, Y. Xu, C. Zhang, D. Wong, J. Liu, X. Cao, Disc aware ensemble network for glaucoma screening from fundus image, IEEE Transactions on Medical Imaging.

41. A. Chakravarty, J. Siv Swamy, A deep learning based joint segmentation and classification framework for glaucoma assessment in retinal colour fundus images, arXivpreprintarXiv:1808.01355.

42. H. Muhammad, T. Fuchs, N. De Coir, C. De Moraes, D. Blumberg, J. Liebmann, R. Ritch, D. Hood, Hybrid deep learning on single wide-field optical coherence tomography scans accurately classifies glaucoma suspects, Journal of glaucoma 26 (12) (2017) 1086-1094.

43. L Hexi, Y He, S Keel, W Meng, RT Chang, and M He. Efficacy of a deep learning system for detecting glaucomatous optic neuropathy based on colour fundus photographs. Ophthalmology, 125(8):1199-1206, Aug 2018.

44. G. C. Chan, R. Kemble, H. Muller, S. Shah, T. Tang, F. Meriaudeau, Fusing results of several deep learning architectures for automatic classification of normal and diabetic macular edema in optical coherence tomography, in: 2018 40th Annual International Conference of the IEEE37Engineering in Medicine and Biology Society (EMBC), IEEE, 2018, pp. 670-673.

45. H. Fu, Y. Xu, D. Wong, J. Liu, Retinal vessel segmentation via deep learning network and fully-connected conditional random fields, in: Biomedical Imaging (ISBI), 2016 IEEE 13th International Symposium on, IEEE, 2016, pp. 698-701.

46. Y. Guo, Y. Liu, A. Oerlemans, S. Lao, S. Wu, M. S. Lew, Deep learning for visual understanding: A review, Neurocomputing 187 (2016) 27-48.

47. M. Niemeijer, B. Van G, M. Cree, A. Mizutani, G. Quellec, C. Sanchez, B. Zhang, R. Hornero, M. Lamard, C. Muramatsu, et al., Retinopathy online challenge: automatic detection of microaneurysms in digital colour fundus photographs, IEEE transactions on medical imaging 29 (1) (2010) 185-195.

48. T. Clemons, E. Chew, S. Bressler, W. McAbee, Age-related eye disease study research, g. national eye institute visual function questionnaire in the age-related eye disease study (areds): Areds report no. 10, Arch Ophthalmol 121 (2) (2003) 211-7.

49. F. Fumiko, S. Alay_on, J. Sanchez, J. Sigut, M. Gonzalez-Hernandez, Rim-one: An open retinal image database for optic nerve evaluation, in: 2011 24th international symposium on computer-based medical systems (CBMS), IEEE, 2011, pp. 1-6.

50. R. Rasti, H. Rabbani, A. Mehridehnavi, F. Hajizadeh, Macular oct classification using a multi-scale convolutional neural network ensemble, IEEE transactions on medical imaging 37 (4) (2018) 1024-1034.

51. M. Jahromi, R. K, H. Rabbani, A. Dehnavi, A. Peyman, F. Hajizadeh, M. Ommani. An automatic algorithm for segmentation of the boundaries of corneal layers in optical coherence tomography images using Gaussian mixture model, Journal of medical signals and sensors 4 (3). (2014) 171.

52. J. Lowell, A. Hunter, D. Steel, A. Basu, R. Ryder, E. Fletcher, L. Kennedy, et al., Optic nerve head segmentation, Medical Imaging, IEEE Transactions on 23 (2) (2004) 256-264.

53. Mookie M.R.K., Acharya U.R., Fujita H., Koh J.E.W., Tan J.H., Chua C.K.,Bhandary S.V., Noronha K., Laude A., Tong L., "Automated detection of age-related macular degeneration using empirical mode decomposition", Knowledge-Based Systems, vol.89, p654–668(2015), DOI: https://doi.org/10.1016/j.knosys.2015.09.012

54. Kanagasingam Y., Bhuiyan A., Abràmoff MD., Smith RT., Goldschmidt L., Wong T.Y., "Progress on retinal image analysis for age related macular degeneration", Progress in Retinal and Eye Research; 38:20-42(2014). doi: 10.1016/j.preteyeres.2013.10.002

55. Haute Autorité de Santé (France), " Dégénérescence maculaire liée à l'âge : prise en charge diagnostique et thérapeutique Méthode (Recommandations pour la pratique clinique), (2012), doi : https://www.hassante.fr/portail/jcms/c_1051619/fr/degenerescence-maculaire-liee-a-l-age-prise-en-charge-diagnostiqueet-therapeutique

56. Association DMLA and Association Retina France, " Dégénérescence maculaire liée à l'âge : Quels sont les symptômes potentiellement évocateurs", (2008), doi : http://www.dmlainfo.fr/modules/DigiOne.DMLA/Client/Books/en-savoir-plus-sur-la-dmla/files/mobile/index.html#6

57. Mookiah M.R.K., Acharya U.R., Fujita H., Koh J.E.W., Tan J.H., Noronha K., Bhandary S.V., Chua C.K., Lim C.M., Laude A., Tong L., "Local configuration pattern features for age-related macular degeneration characterization and classification", Computers in Biology and Medicine, vol.63, p208-218(2015), doi:https://doi.org/10.1016/j.compbiomed.2015.05.019

58. Wong W.L., X., Li X., Cheung C.M., Klein R., Cheng C.Y., Wong T.Y., " Global prevalence of age-related macular degeneration and disease burden projection for 2020 and 2040: a systematic review and meta-analysis", Alancet Global Health, p106-116 (2014), doi: 10.1016/S2214-109X(13)70145-1

59. Sennlaub F., "Dégénérescence maculaire liée à l'âge (DMLA)", doi: https://www.inserm.fr/information-en-sante/dossiers-information/degenerescence-maculaire-liee-agedmla

60. García-Floriano A., Ferreira-Santiago A., Camacho-Nieto O., Yáñez-Márquez C., "A machine learning approach to medical image classification: Detectingage-related macular degeneration in fundus images", Computers and Electrical Engineering, vol.75, p218-229(2019), doi: https://doi.org/10.1016/j.compeleceng.2017.11.008

61. Horta A., Joshi N., Pekala M., Pacheco K.D., Kong J., Bressler N., Freund D.E., Burlina P., " A Hybrid Approach for Incorporating Deep Visual Features and Side Channel Information withApplications to AMD Detection", the 16th IEEE International Conference on Machine Learning and Applications, (2017), doi: https://doi.org/10.1109/ICMLA.2017.00-75

62. Rushkoff D.B., Lamin A., Oakley J.D., Dubis A.M., Sivaprasad S., " Deep Learning for Prediction of AMD Progression: A Pilot Study", Retina, vol. 12, 712-722, (2015), doughty://sci-hub.tw/10.1167/iovs.18-25325

63. Mookie M.R.K., Acharya U.R., Koh J.E.W., Chandran V., Chua C.K., Tan J.H., Lim C.M., Ng E.Y.K.,Noronha K., Tong L., Laude A., "Automated diagnosis of Age-related Macular Degeneration using greyscale features from digital fundus images", Computers in Biology and Medicine, vol. 53, p55–64.(2014), doi:https://doi.org/10.1016/j.compbiomed.2014.07.015

64. Burlina P., Pacheco K.D., Joshi N., Freund D.E., Bressler N.M., "Comparing Humans and Deep Learning Performance for Grading AMD: A Study in Using Universal Deep Features and Transfer Learning for Automated AMD Analysis", Computers in Biology and Medicine, vol. 82, p80-86. (2017), doi: http://sci-hub.tw/10.1016/j.compbiomed.2017.01.018

65. Mittal D. and Kumari K., "Automated detection and segmentation of drusen in retinal fundus images", Computers and Electrical Engineering, vol. 47, p82-95, (2015), delights://doi.org/10.1016/j.compeleceng.2015.08.014

66. Ren X., Zheng Y., Zhao Y., Luo C., Wang H., Lian J., He Y.,"Drusen Segmentation from Retinal Images via Supervised Feature Learning ", IEEE ACCESS, p2952-2961, (2018), doi: https://doi.org/10.1109/ACCESS.2017.2786271

67. Tan J.H., Bhandary S.V., Sivaprasad S., Hagiwara Y., Bagchi A., Raghavendra U., Rao A.K., Raju B., Shetty N.S., Gertych A., Chua K.C., Acharya U.R., "Age-related Macular Degeneration detection using deep convolutional neural network", Future GenerationComputer Systems, vol. 87, 127–135, (2018), doi: https://doi.org/10.1016/j.future.2018.05.001

68. Wang Z., Sadda S.V.R., Hu Z., "Deep learning for automated screening and semantic segmentation of age-related and juvenile atrophic macular degeneration", Proc. SPIE 10950, Medical Imaging 2019: ComputerAided Diagnosis, 109501Q, (2019); doi: 10.1117/12.2511538

69. Burlina P.M., Joshi N., Pekala M., Pacheco K.D., Freund D.E., Bressler N.M., "Automated Grading of Age-Related Macular Degeneration from Colour Fundus Images Using Deep Convolutional Neural Networks", JAMA Ophthalmol, 135:11, 1170-1176, (2017), doi: http://sci-hub.tw/10.1001/jamaophthalmol.2017.3782

70. Liu H., Wong D.W.K., Fu H., Xu Y., Liu J., "DeepAMD: Detect Early Age-Related Macular Degeneration by Applying Deep Learning in a Multiple Instance Learning Framework", ACCV 2018, LNCS 11365, pp. 625–640, (2019), doi : https://doi.org/10.1007/978-3-030-20873-8 _40

71. Ghebrechristos H.E., Alaghband G., Huang R.Y., "Retinet-Features extractor for learning patterns of diabetic retinopathy and Age-Related Macular Degeneration from Publicly available Datasets", international conference on computational science and computational intelligence, (2017), doi:10.1109/CSCI.2017.286

72. Burlina P.M., Joshi N., Pacheco K.D., Freund D.E., Kong J., Bressler N.M., “Use of Deep Learning for De tailed Severity Charac terization and Estimation of 5-Year Risk Among Patients with Age-Related Macular Degeneration”, JAMA Ophthalmology (2018), doi:10.1001/jamaophthalmol.2018.4118

73. Peng Y., Dharssi S., Chen Q., Keenan T.D., Agrón E., Wong W.T., Chew E.Y., Lu Z., “DeepSeeNet: A Deep Learning Model for Automated Classification of Patient-based Age-related Macular Degeneration Severity from Colour Fundus Photographs”, American Academy of Ophthalmology, ISSN 0161-6420/18, doi://doi.org/10.1016/j.ophtha.2018.11.015

74. Grassmann F., Mengelkamp J., Brandl C., Harsch S., Zimmermann M.E., Linkohr B., Peters A., Heid I.M., Palm C., Weber B.H.F., “A Deep Learning Algorithm for Prediction of Age-Related Eye Disease StudySeverity Scale for Age-Related Macular Degeneration from Color Fundus Photography”, American A cademy of Ophthalm ology, ISSN 0161-6420/18, doi: https://doi.org/10.1016/j.ophtha.2018.02.037

75. Z. Hu, Z. Wang, S. Sadda, “Automated segmentation of geographic atrophy using deep convolutional neural networks”, Proceedings Volume 10575, SPIE Medical Imaging 2018: Computer Aided Diagnosis, 1057511 (2018), doi: 10.1117/12.2287001 10.1001/jamaophthalmol.2017.3782

76. Wilkinson CP, Ferris FL, Klein RE, Lee PP, Agardh CD, Davis M, Dills D, Kampik A, Pararajasegaram R, Verdaguer JT. Proposed international clinical diabetic retinopathy and diabetic macular enema disease severity scales. Ophthalmology. 2003 Sep;110(9):1677-82.

77. Harry Pratt, Frans Coenen, Deborah M Broadbent, Simon P Harding, Yalin Zheng. Convolutional Neural Networks for Diabetic Retinopathy. International Conference on Medical Imaging Understanding and Analysis 2016, MIUA 2016, 6-8 July 2016, Loughborough, UK

78. Zhuang Wang, Jianbo Yang. Diabetic Retinopathy Detection via Deep Convolutional Networks for Discriminative Localization and Visual Explanation. Computer Vision and Pattern Recognition, 2017.

79. Bole Zhou, Aditya Khosla, Agata Lapedriza, Aude Oliva, Antonio Torralba. Learning Deep Features for Discriminative Localization. Computer Vision and Pattern Recognition. December. 2016. arXiv: 1512.041150.

80. M. D. Abramoff, Y. Lou, A. Erginay, W. Clarida, R. Amelon, J. C. Folk, and M. Niemeijer. Improved automated detection of diabetic retinopathy on a publicly available dataset through integration of deep learning. Investigative ophthalmology & visual science, 57(13):5200–5206, 2016.

81. Hidenori Takahashi, Hironobu Tampo, Yusuke Arai, Yuji Inoue, Hidetoshi Kawashima. Applying artificial intelligence to disease staging: Deep learning for improved staging of diabetic retinopathy. PLOS ONE | https://doi.org/10.1371/journal.pone.0179790 June 22, 2017

82. Kele Xu, Dawei Feng, Haibo Mi. Deep Convolutional Neural Network-Based Early Automated Detection of Diabetic Retinopathy Using Fundus Image. Molecules 2017, 22, 2054; doi: 10.3390/molecules22122054

83. Jordi de la Torre, Aida Valls, Domenec Puig. A deep learning interpretable classifier for diabetic retinopathy disease grading. Neurocomputing (IF 4.072) Pub Date : 2019-04-24 , DOI: 10.1016/j.neucom.2018.07.102

84. Wei Zhang, Jie Zhong, Shijun Yang, Zhentao Gao, Junjie Hu, Yuanyuan Chen, Zhang Yi Automated identification and grading system of diabetic retinopathy using deep neural networks. Knowledge-Based Systems 175 (2019) 12–25

85. D. Jude Hemanth, Omer Depreciable, UtkuKose. An enhanced diabetic retinopathy detection and classification approach using deep convolutional neural network. Neural Computing and Applications https://doi.org/10.1007/s00521-018-03974-0. Received: 25 September 2018 / Accepted: 20 December 2018. Springer-Verlag London Ltd., part of Springer Nature 2019

86. Rory Sayres, Naama Hammel, Derek Wu, Jesse Smith, Ankur Taly, Ehsan Rahimy, Jonathan Krause, Shawn Xu, Scott Barb, Arjun B. Sood, Katy Blumer, Arunachalam Narayanaswamy, Anthony Joseph, Greg S. Corrado, David Coz, Zahra Rastegar, Michael Shumski, Lily Peng, Dale R. Webster. Using a Deep Learning Algorithm and Integrated Gradients Explanation to Assist Grading for Diabetic Retinopathy. Ophthalmology 2019; 126:552-564 ª 2018 by the American Academy of Ophthalmology. This is an open access article under the CC BY-NC-ND license (http://creativecommons.org/licenses/by-nc-nd/4.0/).

87. Sivaji Dutta, Bonthala CS Manideep, Syed Muzamil Basha, Ronnie D. Caytiles, N. Ch. S. N. Iyengar. Classification of Diabetic Retinopathy Images by Using Deep Learning Models. International Journal of Grid and Distributed Computing Vol. 11, No. 1 (2018), pp.89-106 http://dx.doi.org/10.14257/ijgdc.2018.11.1.09

88. Kang Zhou, Zaiwang Gu, Wen Liu, Weixin Luo, Jun Cheng, Shenghua Gao, Jiang Liu. Multi-Cell Multi-Task Convolutional Neural Networks for Diabetic Retinopathy Grading.

89. Jordi de la Torre, Aida Valls, Domenec Puig. A deep learning interpretable classifier for diabetic retinopathy disease grading. Neurocomputing, https://doi.org/10.1016/j.neucom.2018.07.102

90. Pratap T.L., Kokil P.K., "Computer-aided diagnosis of cataract using deep transfer learning", Biomedical Signal Processing and Control, vol.53, 101533, (2019), doi: https://doi.org/10.1016/j.bspc.2019.04.010

91. Cao L., Li H., Zhang Y., Zhang L., Xu L., "Hierarchical method for cataract grading based on retinal images using improved Haar wavelet", Information Fusion, vol. 53, 196–208, (2020), doi: https://doi.org/10.1016/j.inffus.2019.06.022

92. Zhang L., Li J., Zhang I., Han H., Liu B., Yang J., Wang Q., "Automatic Cataract Detection And Grading Using Deep Convolutional Neural Network", 2017 IEEE 14th International Conference on Networking, Sensing and Control (ICNSC), (2017), Calabria, Italy, doi: https://doi.org/10.1109/ICNSC.2017.8000068

93. Gao X., Lin S., Wong T.Y., "Automatic Feature Learning to Grade Nuclear Cataracts Based on Deep Learning", in Proc. ACCV, (2014).

94. Gao X., Lin S., Wong T.Y., "Automatic Feature Learning to Grade Nuclear Cataracts Based on Deep Learning", IEEE Transactions on Biomedical Engineering, Volume: 62 , Issue: 11 , Nov. 2015, doi : 10.1109/TBME.2015.2444389

95. Amy Ruomei Wu, Samiksha Fouzdar-Jain, Donny W. Suh, « Comparison Study of Funduscopic Examination Using a Smartphone-Based Digital Ophthalmoscope and the Direct Ophthalmoscope », Journal of Pediatric Ophthalmology & Strabismus, Vol. 55, No. 3, 2018.

96. Mehrdad Mohammadpour, Zahra Heidari, Masoud Mirghorbani, Hassan Hashemi, « Smartphones, tele-ophthalmology, and VISION 2020 », Int J Ophthalmol, 2017, Vol. 10, No. 12.doi: 10.18240/ijo.2017.12.19

97. Kai Jin, Haitong Lu, ZhaoanSu, Chuming Cheng, Juan Ye and Dahong Qian, « Telemedicine screening of retinal diseases with a handheld portable non-mydriatic fundus camera », BMC Ophthalmology (2017) 17:89, DOI 10.1186/s12886-017-0484-5

98. Brian C. Toy, David J. Myung, Lingmin He, Carolyn K. Pan, Robert T. Chang, Alison Polkinhorne, Douglas Merrell, Doug Foster, MarkS. Blumenkranz. Smartphone-Based Dilated Fundus Photography and Near Visual Acuity Testing as Inexpensive Screening Tools to Detect Referral Warranted Diabetic Eye Disease. In RETINA 36(5):1, the journal of retinal and vitreaous diseases. 2016.

99. Andrea Russo, William Mapham, Raffaele Turano, Ciro Costagliola, Francesco Morescalchi, NicoloScaroni, and Francesco Semeraro, « Comparison of Smartphone Ophthalmoscopy with Slit Lamp Biomicroscopy for Grading Vertical Cup-to-Disc Ratio », J Glaucoma, Volume 25, Number 9, September 2016.doi: 10.1097/IJG.0000000000000499.

100. Thomas SM, Jeyaraman MM, Hodge WG, Hutnik C, Costella J, Malvankar-Mehta MS. The effectiveness of teleglaucoma versus inpatient examination for glaucoma screening: a systematic review and meta-analysis. PLoS One 2014;9(12): e113779

101. Martha E. Ryan, Ramachandran Rajalakshmi, VijayaraghavanPrathiba, Ranjit Mohan Anjana, Harish Ranjani, K.M. Venkat Narayan, Timothy W. Olsen, Viswanathan Mohan, Laura A. Ward, Michael J. Lynn, Andrew M. Hendrick, « Comparison Among Methods of Retinopathy Assessment (CAMRA) Study », Ophthalmology, 2015 Oct;122(10):2038-43. doi: 10.1016/j.ophtha.2015.06.011.

102. Y. Elloumi, M. Akil, N. Kehtarnavaz. A Computational Efficient Retina Detection and Enhancement Image Processing Pipeline for Smartphone-Captured Fundus Images. Journal of Multimedia Information System.

103. Y. Elloumi, M. Akil, N. Kehtarnavaz. A mobile computer aided system for optic nerve head detection", Computer Methods and Programs in Biomedicine (CMPB), Vol. 162, August 2018, pages 139-148, DOI : https://doi.org/10.1016/j.cmpb.2018.05.004

104. Ramachandran Rajalakshmi, Subramanian Arulmalar, Manoharan Usha, Vijayaraghavan Prathiba, Khaji Syed Kareemuddin, Ranjit Mohan Anjana, Viswanathan

105. Mohan, « Validation of Smartphone Based Retinal Photography for Diabetic Retinopathy Screening », PLoS ONE 10(9): e0138285. doi: 10.1371/journal.pone.0138285

106. M. Lorenza Muiesan, Massimo Salvetti, Anna Paini, Michela Riviera, Clara Pintossi, Fabio Bertacchini, Efrem Colonetti, Claudia Agabiti-Rosei, Maurizio Poli, Francesco Semeraro,Enrico Agabiti-Rosei, and Andrea Russo, « Ocular fundus photography with a Smartphone device inacute hypertension », Journal of Hypertension 2017, 35:1660–1665, Volume 35 Number 8 August 2017.doi: 10.1097/HJH.0000000000001354.

107. Avinash V. Varadarajan, Reena Chopra, RyanPoplin, Pearse A. Keane, Katy Blumer, Greg S. Corrado, Christof Angermueller, Lily Peng, Joe Ledsam, Dale R. Webster. Deep Learning for Predicting Refractive Error From Retinal Fundus Images. IOVS, June 2018, Vol. 59, No. 7, 2862

108. Ramachandran Rajalakshmi, Radhakrishnan Subashini, Ranjit Mohan Anjana, Viswanathan Mohan. Automated diabetic retinopathy detection in Smartphone-based fundus photography using artificial intelligence. Eye (2018) 32:1138–144https://doi.org/10.1038/s41433-018-0064-9.

109. Haoran Wei; Abhishek Sehgal; Nasser Kehtarnavaz. A deep learning-based Smartphone app for real-time detection of retinal abnormalities in fundus images. Proc. SPIE 10996, Real-Time Image Processing and Deep Learning 2019, 1099602 (14 May 2019); doi:10.1117/12.2516665

110. Bolster NM, Giardini ME, Livingstone IAT, Bastawrous A. How the Smartphone is driving the eye-health imaging revolution. Expert Rev Ophthalmology. 2014; 9:475–485.

111. Basitarsus A, Rono HK, Livingstone IAT, et al. Development and validation of a Smartphone-based visual acuity test (peek acuity) for clinical practice and community-based field work. JAMA Ophthalmology. 2015; 133:930–937.

112. P. Burkina, D. E. Freund, N. Joshi, Y. Wolfson, N. M. Bressler, “Detection of Age-related of macular degeneration via Deep Learning”, 2016 IEEE 13th International Symposium on Biomedical Imaging (ISBI)(2016), 184 – 188, DOI:10.1109/ISBI.2016.7493240

113. P. Burlina, D. E. Freund, N. Joshi, Y. Wolfson, N. M. Bressler, “Comparing Humans and Deep Learning Performance for Grading AMD: A Study in Using Universal Deep Features and Transfer Learning for Automated AMD Analysis”, Computer in Biology and Medicine, Volume 82, 1 March 2017, Pages 80-86, DOI: https://doi.org/10.1016/j.compbiomed.2017.01.018